SIAM J. Imaging Sciences
Vol. 17, No. 4, pp. 2142–2173

The Linear Sampling Method for Data Generated by Small Random Scatterers*

Josselin Garnier†, Houssem Haddar‡, and Hadrien Montanelli‡

Abstract. We present an extension of the linear sampling method for solving the sound-soft inverse scattering problem in two dimensions with data generated by randomly distributed small scatterers. The theoretical justification of our novel sampling method is based on a rigorous asymptotic model, a modified Helmholtz–Kirchhoff identity, and our previous work on the linear sampling method for random sources. Our numerical implementation incorporates boundary elements, singular value decomposition, Tikhonov regularization, and Morozov's discrepancy principle. We showcase the robustness and accuracy of our algorithms with a series of numerical experiments.

Key words. inverse acoustic scattering problem, Helmholtz equation, linear sampling method, passive imaging, singular value decomposition, Tikhonov regularization, ill-posed problems

MSC codes. 35J05, 35R30, 35R60, 65M30, 65M32

DOI. 10.1137/24M1650417

1. Introduction.

Inverse scattering problems arise across a multitude of fields, ranging from medical imaging and nondestructive testing to radar technology and seismology. At their core, these problems involve the task of deducing the characteristics of an object or medium from the scattered signals it generates. These problems involve several challenges, including nonlinearity, which is particularly pronounced near resonance, making linearization inapplicable; these are also severely ill-posed, raising questions about uniqueness and stability, and necessitating the inclusion of regularization. Additionally, for iterative procedures, reconstruction time can be lengthy and prior knowledge is required for initialization. In this context, fast, data-driven algorithms, such as the linear sampling method (LSM), can be useful in reducing computational costs [10, 11, 14] and initializing more sophisticated algorithms [6]. For an exploration of the history and evolution of the LSM, readers can refer to the 2018 *SIAM Review* article by Colton and Kress [12]. Further mathematical insights can be found in dedicated books [7, 8, 13]; recent developments include the generalized LSM, in both full- and limited-aperture measurements [3, 4].

Two acquisition configurations are commonly used in inverse scattering problems—active and passive. Active imaging involves sending waves through *controlled* sources and recording the medium's response through *controlled* sensors. Passive imaging, on the other hand, employs controlled sensors but relies on *random, uncontrolled* sources (such as microseisms and

*Received by the editors March 28, 2024; accepted for publication (in revised form) July 5, 2024; published electronically October 21, 2024.
https://doi.org/10.1137/24M1650417
Funding: The work of the authors was partially supported by the Agence de l'Innovation de Défense (AID) via Centre Interdisciplinaire d'Études pour la Défense et la Sécurité (CIEDS) project PRODIPO.
†CMAP, École Polytechnique, IP Paris, 91120 Palaiseau, France (josselin.garnier@polytechnique.edu).
‡Inria, UMA, ENSTA Paris, IP Paris, 91120 Palaiseau, France (houssem.haddar@inria.fr, hadrien.montanelli@inria.fr).

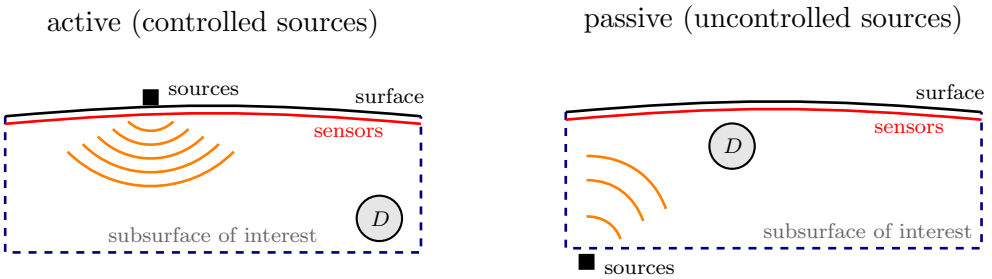

Figure 1. *In subsurface imaging, the objective is to capture an image of a specific subsurface area to identify a defect, denoted as D—this could involve, for instance, locating shallow or deep geothermal reservoirs. In active imaging (on the left), both the sources and sensors are controlled. Vibroseismic trucks on the surface can generate signals, and sensors can be strategically placed and moved as desired. In passive imaging (on the right), controlled sensors are still utilized, but the signal originates from uncontrolled, random sources within the subsurface, such as microseisms and ocean swells.*

ocean swells in seismology). In this setup, it is the cross-correlations between the recorded signals that convey information about the medium [19, 21]. Passive imaging is a rapidly growing research topic because it enables the imaging of areas where the use of active sources is not possible due to, e.g., safety or environmental reasons. Additionally, even in scenarios where active sources could be employed, utilizing passive sources helps reduce operational costs and enhances stealth in defense applications. Other applications encompass crystal tomography and seismic interferometry for volcano monitoring [22, 28]. Passive imaging has also demonstrated success in other fields, including structural health monitoring [15, 27], oceanography [20, 29, 32], and medical elastography [17]. We illustrate active and passive imaging in the context of subsurface imaging in Figure 1.

In a previous paper [18], we introduced an extension of the LSM to address the sound-soft inverse scattering problem involving random sources. This current study builds upon that foundation, focusing on a scenario where a single *controlled* source, operating at a specified wavelength λ, illuminates a small *random* scatterer and an object of comparable size to λ—our goal is to reconstruct the shape of the latter. The reflection of the wave field transmitted by the point source on the small scatterer serves as a random source, aligning with the context explored in our earlier work. The motivation for this research stems from the necessity, when imaging an unknown obstacle D, to illuminate it with a diverse set of incoming waves. For deterministic, controlled point sources in two dimensions, one considers a family of sources located at points $\boldsymbol{z}_m$ generating the incident fields

$$\phi(\boldsymbol{x}, \boldsymbol{z}_m) = \frac{i}{4} H_0^{(1)}(k|\boldsymbol{x} - \boldsymbol{z}_m|) \tag{1.1}$$

and measures the resulting scattered fields $u^s(\boldsymbol{x}_j, \boldsymbol{z}_m)$ at points $\boldsymbol{x}_j$ to populate the near-field matrix N with entries $N_{jm} = u^s(\boldsymbol{x}_j, \boldsymbol{z}_m)$. In the case of random, uncontrolled sources at positions $\boldsymbol{z}_\ell$, as demonstrated in our prior work [18], the relevant matrix is the cross-correlation matrix C. Its entries are given by

$$C_{jm} = \frac{2ik|\Sigma|}{L} \sum_{\ell=1}^{L} \overline{u(\boldsymbol{x}_j, \boldsymbol{z}_\ell)} u(\boldsymbol{x}_m, \boldsymbol{z}_\ell) - \left[\phi(\boldsymbol{x}_j, \boldsymbol{x}_m) - \overline{\phi(\boldsymbol{x}_j, \boldsymbol{x}_m)}\right], \tag{1.2}$$

where $u(\boldsymbol{x},\boldsymbol{z}) = \phi(\boldsymbol{x},\boldsymbol{z}) + u^s(\boldsymbol{x},\boldsymbol{z})$ is the total field for the incident wave $\phi(\boldsymbol{x},\boldsymbol{z})$, and $|\Sigma|$ is the area of the surface Σ on which the random sources are distributed. (Note that it is not necessary to know or estimate the positions $\boldsymbol{z}_\ell$ to assemble the matrix C.)

Suppose now that we only have a single *controlled* source located at a given point $\boldsymbol{z}$, as opposed to several positions $\boldsymbol{z}_m$. This is insufficient for reconstructing the obstacle's shape with the LSM (the near-field matrix N would have rank one). To address this limitation, we propose introducing a random medium between the source and the obstacle. We illustrate this concept, in acoustic scattering, by considering a single small random scatterer between the source and the obstacle—a seemingly simple yet powerful model of a random medium that allows us to apply the LSM in a novel manner, with a modified version of (1.2). The extension to elastic waves in subsurface imaging will be the subject of future work.

Our method is supported by various key components, such as a rigorous asymptotic model (see section 2) and a *modified* Helmholtz–Kirchhoff identity (discussed in section 3). The paper explores numerical implementations, utilizing boundary elements alongside singular value decomposition (SVD), Tikhonov regularization, and Morozov's discrepancy principle (detailed in section 4). A set of numerical experiments is presented in the same section, offering valuable insights into the practical applications of our research.

2. Asymptotic model.

Mathematically, the configuration described in the introduction unfolds as follows. Consider the incident field (1.1) generated by a point source located at $\boldsymbol{z}_\epsilon = \lambda\epsilon^{-q}e^{i\theta_z}$ for some scalars $q > 0$ and $\theta_z \in [0, 2\pi]$. (Complex variables will be employed to determine the coordinates of points in the plane.) Here, $\epsilon > 0$ is a small dimensionless parameter, $k > 0$ is the wavenumber, and $\lambda = 2\pi/k$ is the wavelength, which we assume to be independent of ϵ. Let D be an obstacle of size proportional to λ and independent of ϵ, i.e., there exists a constant $C > 0$ such that its radius verifies $\rho(D) = \frac{1}{2}\sup_{\boldsymbol{x},\boldsymbol{y}\in D}|\boldsymbol{x}-\boldsymbol{y}| = C\lambda$. Without loss of generality, we assume that the geometric center of the obstacle D is at the origin. We also consider a small disk $D_\epsilon = D_\epsilon(\boldsymbol{y}_\epsilon)$ of radius $\rho(D_\epsilon) = \lambda\epsilon$ centered at $\boldsymbol{y}_\epsilon = \lambda\epsilon^{-p}e^{i\theta_y}$ for some scalars $0 < p < q$ and $\theta_y \in [0, 2\pi]$.[1] Finally, let $B \subset \mathbb{R}^2 \setminus \overline{D \cup D_\epsilon}$ be a compact set whose size and distance to D are proportional to λ and independent of ϵ, i.e., $\rho(B) \propto \lambda$ and $d(B, D) = \inf_{\boldsymbol{x}\in B,\,\boldsymbol{y}\in D}|\boldsymbol{x}-\boldsymbol{y}| \propto \lambda$. Measurements will be taken inside the volume B, which is consistent with [18]. We also assume that ∂D and ∂B are smooth enough to allow the forming of Dirichlet and Neumann traces and the application of partial integration formulas (Lipschitz continuity is a sufficient condition). To summarize, we make the following assumptions (see also Figure 2):[2]

$$\begin{aligned} &\boldsymbol{y}_\epsilon = \lambda\epsilon^{-p}e^{i\theta_y}, \quad \boldsymbol{z}_\epsilon = \lambda\epsilon^{-q}e^{i\theta_z}, \quad 0 < p < q, \\ &\rho(D),\, \rho(B),\, d(B,D) = \mathcal{O}(1), \quad \rho(D_\epsilon) = \mathcal{O}(\epsilon). \end{aligned} \tag{2.1}$$

We examine the scattering of the incident field $\phi(\cdot, \boldsymbol{z}_\epsilon)$ by D and D_ϵ, which generates the scattered field w_ϵ^s. More precisely, let $w_\epsilon^s(\cdot, \boldsymbol{y}_\epsilon, \boldsymbol{z}_\epsilon) \in H^1_{\mathrm{loc}}(\mathbb{R}^2 \setminus \{D \cup D_\epsilon\})$ be the solution to the sound-soft scattering problem

[1] Throughout the paper, we will assume that k^2 is not a Dirichlet eigenvalue of $-\Delta$ in both D and D_ϵ. For the latter, this assumption is always verified for small enough ϵ.

[2] We recall that $f(\epsilon) = \mathcal{O}(\epsilon)$ means that there exists a constant $C > 0$, independent of ϵ, such that for small enough ϵ, $|f(\epsilon)| \le C\epsilon$.

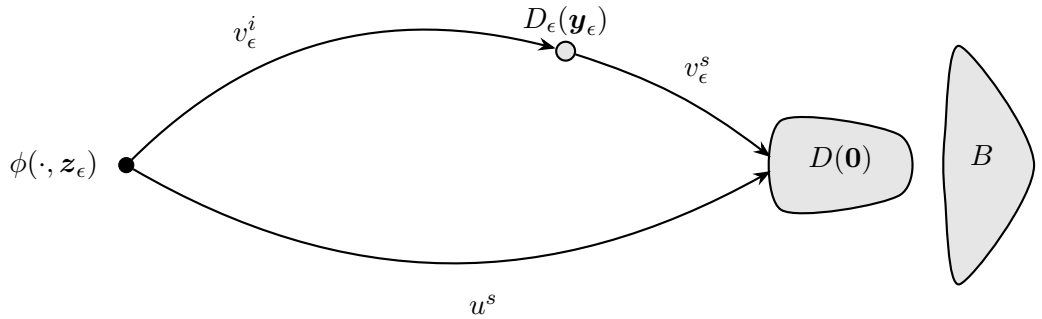

Figure 2. *The incident field $\phi(\cdot,\boldsymbol{z}_\epsilon)$ is generated by a point source located at $\boldsymbol{z}_\epsilon=\lambda\epsilon^{-q}e^{i\theta_z}$. It is scattered by a small disk D_ϵ of radius $\mathcal{O}(\epsilon)$ centered at $\boldsymbol{y}_\epsilon=\lambda\epsilon^{-p}e^{i\theta_y}$ and an obstacle D of radius $\mathcal{O}(1)$ centered at the origin. Measurements are taken near the obstacle D in a volume B, whose size is also $\mathcal{O}(1)$. The resulting scattered field, w_ϵ^s, can be approximated with an error $\mathcal{O}(|\log\epsilon|^{-1}\epsilon^p\epsilon^{q/2})$ in the $H^1(B)$-norm by the three-term sum $u^s+v_\epsilon^i+v_\epsilon^s$. As $\epsilon\to 0$, the radius of D_ϵ goes to 0, and $\boldsymbol{y}_\epsilon$ and $\boldsymbol{z}_\epsilon$ shoot to infinity. The scattering sequences, along with the amplitudes of the scattered fields, are also shown in Table 1.*

$$\begin{cases}\Delta w_\epsilon^s(\cdot,\boldsymbol{y}_\epsilon,\boldsymbol{z}_\epsilon)+k^2w_\epsilon^s(\cdot,\boldsymbol{y}_\epsilon,\boldsymbol{z}_\epsilon)=0 \quad \text{in } \mathbb{R}^2\setminus\{\overline{D\cup D_\epsilon}\},\\ w_\epsilon^s(\cdot,\boldsymbol{y}_\epsilon,\boldsymbol{z}_\epsilon)=-\phi(\cdot,\boldsymbol{z}_\epsilon) \quad \text{on } \partial D\cup\partial D_\epsilon,\\ w_\epsilon^s(\cdot,\boldsymbol{y}_\epsilon,\boldsymbol{z}_\epsilon) \text{ is radiating.}\end{cases} \tag{2.2}$$

Note that the (Sommerfeld) radiation condition in (2.2) reads

$$\lim_{|\boldsymbol{x}|\to\infty}\sqrt{|\boldsymbol{x}|}\left(\frac{\boldsymbol{x}}{|\boldsymbol{x}|}\nabla_{\boldsymbol{x}}w_\epsilon^s(\boldsymbol{x},\boldsymbol{y}_\epsilon,\boldsymbol{z}_\epsilon)-ikw_\epsilon^s(\boldsymbol{x},\boldsymbol{y}_\epsilon,\boldsymbol{z}_\epsilon)\right)=0, \quad \text{(uniformly in } \boldsymbol{x}/|\boldsymbol{x}|). \tag{2.3}$$

The condition (2.3) ensures that the solution represents an outgoing wave.

We shall show that $w_\epsilon^s(\cdot,\boldsymbol{y}_\epsilon,\boldsymbol{z}_\epsilon)$ can be approximated as the sum of three terms,

$$w_\epsilon^s(\cdot,\boldsymbol{y}_\epsilon,\boldsymbol{z}_\epsilon)\approx u^s(\cdot,\boldsymbol{z}_\epsilon)+v_\epsilon^i(\cdot,\boldsymbol{y}_\epsilon,\boldsymbol{z}_\epsilon)+v_\epsilon^s(\cdot,\boldsymbol{y}_\epsilon,\boldsymbol{z}_\epsilon) \tag{2.4}$$

with an error $\mathcal{O}(|\log\epsilon|^{-1}\epsilon^p\epsilon^{q/2})$ in the $H^1(B)$-norm; the scattered fields in the expansion above, $u^s(\cdot,\boldsymbol{z}_\epsilon)\in H^1_{\text{loc}}(\mathbb{R}^2\setminus D)$, $v_\epsilon^i(\cdot,\boldsymbol{y}_\epsilon,\boldsymbol{z}_\epsilon)\in H^1_{\text{loc}}(\mathbb{R}^2\setminus D_\epsilon)$, and $v_\epsilon^s(\cdot,\boldsymbol{y}_\epsilon,\boldsymbol{z}_\epsilon)\in H^1_{\text{loc}}(\mathbb{R}^2\setminus D)$, are the solutions to the sound-soft scattering problems

$$\begin{cases}\Delta u^s(\cdot,\boldsymbol{z}_\epsilon)+k^2u^s(\cdot,\boldsymbol{z}_\epsilon)=0 \quad \text{in } \mathbb{R}^2\setminus\overline{D},\\ u^s(\cdot,\boldsymbol{z}_\epsilon)=-\phi(\cdot,\boldsymbol{z}_\epsilon) \quad \text{on } \partial D,\\ u^s(\cdot,\boldsymbol{z}_\epsilon) \text{ is radiating,}\end{cases} \tag{2.5}$$

$$\begin{cases}\Delta v_\epsilon^i(\cdot,\boldsymbol{y}_\epsilon,\boldsymbol{z}_\epsilon)+k^2v_\epsilon^i(\cdot,\boldsymbol{y}_\epsilon,\boldsymbol{z}_\epsilon)=0 \quad \text{in } \mathbb{R}^2\setminus\overline{D_\epsilon},\\ v_\epsilon^i(\cdot,\boldsymbol{y}_\epsilon,\boldsymbol{z}_\epsilon)=-\phi(\cdot,\boldsymbol{z}_\epsilon) \quad \text{on } \partial D_\epsilon,\\ v_\epsilon^i(\cdot,\boldsymbol{y}_\epsilon,\boldsymbol{z}_\epsilon) \text{ is radiating,}\end{cases} \tag{2.6}$$

and

$$\begin{cases}\Delta v_\epsilon^s(\cdot,\boldsymbol{y}_\epsilon,\boldsymbol{z}_\epsilon)+k^2v_\epsilon^s(\cdot,\boldsymbol{y}_\epsilon,\boldsymbol{z}_\epsilon)=0 \quad \text{in } \mathbb{R}^2\setminus\overline{D},\\ v_\epsilon^s(\cdot,\boldsymbol{y}_\epsilon,\boldsymbol{z}_\epsilon)=-v_\epsilon^i(\cdot,\boldsymbol{y}_\epsilon,\boldsymbol{z}_\epsilon) \quad \text{on } \partial D,\\ v_\epsilon^s(\cdot,\boldsymbol{y}_\epsilon,\boldsymbol{z}_\epsilon) \text{ is radiating.}\end{cases} \tag{2.7}$$

We illustrate the scattering problems (2.2) and (2.5)–(2.7) in Figure 2.

We start by proving estimates on $u^s(\cdot, \boldsymbol{z}_\epsilon)$, which corresponds to the wave field transmitted by the point source $\phi(\cdot, \boldsymbol{z}_\epsilon)$ scattered by D alone.

Lemma 2.1 (estimates on u^s). *There exists a constant $C > 0$, independent of ϵ, such that for small enough ϵ,*

$$\|u^s(\cdot, \boldsymbol{z}_\epsilon)\|_{H^1(B)} \le C\epsilon^{q/2} \tag{2.8}$$

and

$$\|u^s(\cdot, \boldsymbol{z}_\epsilon)\|_{H^{1/2}(\partial D_\epsilon)} \le C\epsilon^{p/2}\epsilon^{q/2}. \tag{2.9}$$

Proof. We write $u^s(\cdot, \boldsymbol{z}_\epsilon) = Sg(\cdot, \boldsymbol{z}_\epsilon)$ on ∂D with the single layer operator

$$\begin{aligned} &S : H^{-1/2}(\partial D) \to H^{1/2}(\partial D), \\ &Sg(\boldsymbol{x}) = \int_{\partial D} \phi(\boldsymbol{x}, \boldsymbol{y}) g(\boldsymbol{y}) ds(\boldsymbol{y}), \quad \boldsymbol{x} \in \partial D. \end{aligned} \tag{2.10}$$

Once we solve $Sg(\cdot, \boldsymbol{z}_\epsilon) = -\phi(\cdot, \boldsymbol{z}_\epsilon)$ for the surface density $g(\cdot, \boldsymbol{z}_\epsilon)$, the solution in B reads $u^s(\cdot, \boldsymbol{z}_\epsilon) = \mathscr{S} g(\cdot, \boldsymbol{z}_\epsilon) = -\mathscr{S} S^{-1} \phi(\cdot, \boldsymbol{z}_\epsilon)$ with

$$\begin{aligned} &\mathscr{S} : H^{-1/2}(\partial D) \to H^1(B), \\ &\mathscr{S} g(\boldsymbol{x}) = \int_{\partial D} \phi(\boldsymbol{x}, \boldsymbol{y}) g(\boldsymbol{y}) ds(\boldsymbol{y}), \quad \boldsymbol{x} \in B. \end{aligned} \tag{2.11}$$

Using the continuity of the operators $\mathscr{S}$ (see Lemma B.1) and S^{-1}, and asymptotics for large arguments of Hankel functions (see Lemma C.3), we obtain, for small enough ϵ,

$$\|u^s(\cdot, \boldsymbol{z}_\epsilon)\|_{H^1(B)} \le \|\mathscr{S}\| \, \|S^{-1}\| \, \|\phi(\cdot, \boldsymbol{z}_\epsilon)\|_{H^{1/2}(\partial D)} \le C\epsilon^{q/2}, \tag{2.12}$$

with a constant C independent of ϵ.[3]

For the second inequality, the solution reads $u^s(\cdot, \boldsymbol{z}_\epsilon) = -T_\epsilon^T S^{-1} \phi(\cdot, \boldsymbol{z}_\epsilon)$ on ∂D_ϵ with

$$\begin{aligned} &T_\epsilon^T : H^{-1/2}(\partial D) \to H^{1/2}(\partial D_\epsilon), \\ &T_\epsilon^T g(\boldsymbol{x}) = \int_{\partial D} \phi(\boldsymbol{x}, \boldsymbol{y}) g(\boldsymbol{y}) ds(\boldsymbol{y}), \quad \boldsymbol{x} \in \partial D_\epsilon. \end{aligned} \tag{2.13}$$

Using the estimate for T_ϵ^T in Lemma B.1, we arrive at

$$\|u^s(\cdot, \boldsymbol{z}_\epsilon)\|_{H^{1/2}(\partial D_\epsilon)} \le \|T_\epsilon^T\| \, \|S^{-1}\| \, \|\phi(\cdot, \boldsymbol{z}_\epsilon)\|_{H^{1/2}(\partial D)} \le C\epsilon^{p/2}\epsilon^{q/2}. \tag{2.14}$$

■

We interpret the estimates in Lemma 2.1 as follows. The small norm of $u^s(\cdot, \boldsymbol{z}_\epsilon)$ can be attributed to the wave field transmitted by the point source covering a distance $d = \mathcal{O}(\epsilon^{-q})$ to reach D, with its amplitude decaying as $1/\sqrt{d}$. Subsequently, during the evaluation in the proximity of D within B, there is no additional loss of signal amplitude. However, when we evaluate it on ∂D_ϵ, some signal amplitude is lost, as it has to travel back from D to ∂D_ϵ covering a distance of $\mathcal{O}(\epsilon^{-p})$, resulting in an additional decaying term of $\mathcal{O}(\epsilon^{p/2})$.

We continue with estimates on $v_\epsilon^i(\cdot, \boldsymbol{y}_\epsilon, \boldsymbol{z}_\epsilon)$, representing the wave field transmitted by the point source $\phi(\cdot, \boldsymbol{z}_\epsilon)$ scattered solely by $D_\epsilon(\boldsymbol{y}_\epsilon)$.

[3]We will consistently denote all constants independent of ϵ as "C," irrespective of potential variations between inequalities or equalities.

Lemma 2.2 (estimates on v_ϵ^i). *The solution to* (2.6) *reads*

$$v_\epsilon^i(\boldsymbol{x},\boldsymbol{y}_\epsilon,\boldsymbol{z}_\epsilon) = -\frac{i}{4}\sum_{n=-\infty}^{+\infty} \frac{H_n^{(1)}(k|\boldsymbol{y}_\epsilon-\boldsymbol{z}_\epsilon|)J_n(2\pi\epsilon)}{H_n^{(1)}(2\pi\epsilon)} e^{-in(\mu_\epsilon+\pi)} H_n^{(1)}(k|\boldsymbol{x}-\boldsymbol{y}_\epsilon|)e^{in\theta} \tag{2.15}$$

in the polar coordinate system $(|\boldsymbol{x}-\boldsymbol{y}_\epsilon|,\theta)$ *centered at* $\boldsymbol{y}_\epsilon$*; the angle* μ_ϵ *is the angle of* $\boldsymbol{y}_\epsilon$ *in the polar coordinate system centered at* $\boldsymbol{z}_\epsilon$*. Moreover, there exists a constant* $C>0$*, independent of* ϵ*, such that for small enough* ϵ*,*

$$\|v_\epsilon^i(\cdot,\boldsymbol{y}_\epsilon,\boldsymbol{z}_\epsilon)\|_{H^1(B)} \le C|\log\epsilon|^{-1}\epsilon^{p/2}\epsilon^{q/2} \tag{2.16}$$

and

$$\|v_\epsilon^i(\cdot,\boldsymbol{y}_\epsilon,\boldsymbol{z}_\epsilon)\|_{H^{1/2}(\partial D)} \le C|\log\epsilon|^{-1}\epsilon^{p/2}\epsilon^{q/2}. \tag{2.17}$$

Proof. We look for a solution of the form

$$v_\epsilon^i(\boldsymbol{x},\boldsymbol{y}_\epsilon,\boldsymbol{z}_\epsilon) = \frac{1}{\sqrt{2\pi}}\sum_{n=-\infty}^{+\infty} \frac{c_n(\epsilon)}{H_n^{(1)}(2\pi\epsilon)} H_n^{(1)}(k|\boldsymbol{x}-\boldsymbol{y}_\epsilon|)e^{in\theta} \tag{2.18}$$

with Fourier coefficients

$$c_n(\epsilon) = \frac{1}{2\pi}\int_0^{2\pi} v_\epsilon^i(\boldsymbol{y}_\epsilon+\lambda\epsilon e^{i\theta},\boldsymbol{y}_\epsilon,\boldsymbol{z}_\epsilon)e^{-in\theta}d\theta. \tag{2.19}$$

We must rewrite the right-hand side of the boundary condition in (2.6). Utilizing Graf's addition theorem (see, e.g., [1, eq. (9.1.79)] or [23, eq. (5.12.11)]), we obtain

$$H_0^{(1)}(k|\boldsymbol{x}-\boldsymbol{z}_\epsilon|) = \sum_{n=-\infty}^{+\infty} H_n^{(1)}(k|\boldsymbol{y}_\epsilon-\boldsymbol{z}_\epsilon|)J_n(k|\boldsymbol{x}-\boldsymbol{y}_\epsilon|)e^{-in(\mu_\epsilon+\pi)}e^{in\theta}. \tag{2.20}$$

Utilizing the boundary condition yields the desired result.

Although a closed-form formula exists for v_ϵ^i, estimating it within B and on ∂D using this formula is quite challenging due to the lack of uniform estimates for the terms of the series. Instead, we write $v_\epsilon^i(\cdot,\boldsymbol{y}_\epsilon,\boldsymbol{z}_\epsilon) = S_\epsilon g_\epsilon(\cdot,\boldsymbol{z}_\epsilon)$ on ∂D_ϵ with the single layer operator

$$\begin{aligned} &S_\epsilon : H^{-1/2}(\partial D_\epsilon) \to H^{1/2}(\partial D_\epsilon),\\ &S_\epsilon g(\boldsymbol{x}) = \int_{\partial D_\epsilon} \phi(\boldsymbol{x},\boldsymbol{y})g(\boldsymbol{y})ds(\boldsymbol{y}), \quad \boldsymbol{x}\in\partial D_\epsilon. \end{aligned} \tag{2.21}$$

The solution in B then reads $v_\epsilon^i(\cdot,\boldsymbol{y}_\epsilon,\boldsymbol{z}_\epsilon) = \mathscr{S}_\epsilon g_\epsilon(\cdot,\boldsymbol{z}_\epsilon) = -\mathscr{S}_\epsilon S_\epsilon^{-1}\phi(\cdot,\boldsymbol{z}_\epsilon)$ with

$$\begin{aligned} &\mathscr{S}_\epsilon : H^{-1/2}(\partial D_\epsilon) \to H^1(B),\\ &\mathscr{S}_\epsilon g(\boldsymbol{x}) = \int_{\partial D_\epsilon} \phi(\boldsymbol{x},\boldsymbol{y})g(\boldsymbol{y})ds(\boldsymbol{y}), \quad \boldsymbol{x}\in B. \end{aligned} \tag{2.22}$$

Using the estimate for $\mathscr{S}_\epsilon$ (see Lemma B.1) and applying Theorem A.3 to $f(\cdot,\boldsymbol{z}_\epsilon)=\phi(\cdot,\boldsymbol{z}_\epsilon)$ with $r=q/2$, we obtain, for small enough ϵ,

$$\|v_\epsilon^i(\cdot,\boldsymbol{y}_\epsilon,\boldsymbol{z}_\epsilon)\|_{H^1(B)} \le \|\mathscr{S}_\epsilon\|\,\|S_\epsilon^{-1}\phi(\cdot,\boldsymbol{z}_\epsilon)\|_{H^{-1/2}(\partial D_\epsilon)} \le C|\log\epsilon|^{-1}\epsilon^{p/2}\epsilon^{q/2} \tag{2.23}$$

with a constant C independent of ϵ.

For the second inequality, the solution reads $v_\epsilon^i(\cdot,\boldsymbol{y}_\epsilon,\boldsymbol{z}_\epsilon)=-T_\epsilon S_\epsilon^{-1}\phi(\cdot,\boldsymbol{z}_\epsilon)$ on ∂D with

$$\begin{aligned} &T_\epsilon : H^{-1/2}(\partial D_\epsilon)\to H^{1/2}(\partial D),\\ &T_\epsilon g(\boldsymbol{x})=\int_{\partial D_\epsilon}\phi(\boldsymbol{x},\boldsymbol{y})g(\boldsymbol{y})ds(\boldsymbol{y}),\quad \boldsymbol{x}\in\partial D. \end{aligned} \tag{2.24}$$

Using the estimate for T_ϵ in Lemma B.1, we arrive at

$$\|v_\epsilon^i(\cdot,\boldsymbol{y}_\epsilon,\boldsymbol{z}_\epsilon)\|_{H^{1/2}(\partial D)} \le \|T_\epsilon\|\,\|S_\epsilon^{-1}\phi(\cdot,\boldsymbol{z}_\epsilon)\|_{H^{-1/2}(\partial D_\epsilon)} \le C|\log\epsilon|^{-1}\epsilon^{p/2}\epsilon^{q/2}. \tag{2.25}$$

■

From Lemma 2.2, we understand that the small norm of $v_\epsilon^i(\cdot,\boldsymbol{y}_\epsilon,\boldsymbol{z}_\epsilon)$ can be explained by the decay of the wave field transmitted by the point source over a distance $d=\mathcal{O}(\epsilon^{-q})$ to reach D_ϵ—the wave field experiences a decay in amplitude proportional to $1/\sqrt{d}$. Subsequently, during the evaluation in the vicinity of D within B and on ∂D, some signal amplitude is lost as the wave travels from D_ϵ to D, covering a distance of $\mathcal{O}(\epsilon^{-p})$, introducing an additional decaying term of $\mathcal{O}(\epsilon^{p/2})$. Last, the presence of the logarithmic term is a consequence of D_ϵ having a radius of $\mathcal{O}(\epsilon)$.

The final step preceding the proof of our main theorem involves deriving estimates for $v_\epsilon^s(\cdot,\boldsymbol{y}_\epsilon,\boldsymbol{z}_\epsilon)$, representing the scattering of $v_\epsilon^i(\cdot,\boldsymbol{y}_\epsilon,\boldsymbol{z}_\epsilon)$ by D.

Lemma 2.3 (estimates on v_ϵ^s). *There exists a constant $C>0$, independent of ϵ, such that for small enough ϵ,*

$$\|v_\epsilon^s(\cdot,\boldsymbol{y}_\epsilon,\boldsymbol{z}_\epsilon)\|_{H^1(B)} \le C|\log\epsilon|^{-1}\epsilon^{p/2}\epsilon^{q/2} \tag{2.26}$$

and

$$\|v_\epsilon^s(\cdot,\boldsymbol{y}_\epsilon,\boldsymbol{z}_\epsilon)\|_{H^{1/2}(\partial D_\epsilon)} \le C|\log\epsilon|^{-1}\epsilon^{p}\epsilon^{q/2}. \tag{2.27}$$

Proof. The first inequality follows from

$$\|v_\epsilon^s(\cdot,\boldsymbol{y}_\epsilon,\boldsymbol{z}_\epsilon)\|_{H^1(B)} \le C\|v_\epsilon^i(\cdot,\boldsymbol{y}_\epsilon,\boldsymbol{z}_\epsilon)\|_{H^{1/2}(\partial D)}, \tag{2.28}$$

a standard result of functional analysis (see, e.g., [16, Chap. 6]). For the second inequality, we write $v_\epsilon^s(\cdot,\boldsymbol{y}_\epsilon,\boldsymbol{z}_\epsilon)=-T_\epsilon^T S^{-1}v_\epsilon^i(\cdot,\boldsymbol{y}_\epsilon,\boldsymbol{z}_\epsilon)$ on ∂D_ϵ, and then

$$\|v_\epsilon^s(\cdot,\boldsymbol{y}_\epsilon,\boldsymbol{z}_\epsilon)\|_{H^{1/2}(\partial D_\epsilon)} \le \|T_\epsilon^T\|\,\|S^{-1}\|\,\|v_\epsilon^i(\cdot,\boldsymbol{y}_\epsilon,\boldsymbol{z}_\epsilon)\|_{H^{1/2}(\partial D)} \le C|\log\epsilon|^{-1}\epsilon^{p}\epsilon^{q/2}. \tag{2.29}$$

■

The amplitude of $v_\epsilon^s(\cdot,\boldsymbol{y}_\epsilon,\boldsymbol{z}_\epsilon)$ in B is the same as that of $v_\epsilon^i(\cdot,\boldsymbol{y}_\epsilon,\boldsymbol{z}_\epsilon)$. However, on ∂D_ϵ, because of the distance $\mathcal{O}(\epsilon^{-p})$, we get an additional decaying factor of $\mathcal{O}(\epsilon^{p/2})$.

Let $e_\epsilon(\cdot,\boldsymbol{y}_\epsilon,\boldsymbol{z}_\epsilon)\in H^1_{\mathrm{loc}}(\mathbb{R}^2\setminus\{D\cup D_\epsilon\})$ be the error

$$e_\epsilon(\cdot,\boldsymbol{y}_\epsilon,\boldsymbol{z}_\epsilon)=w^s_\epsilon(\cdot,\boldsymbol{y}_\epsilon,\boldsymbol{z}_\epsilon)-u^s(\cdot,\boldsymbol{z}_\epsilon)-v^i_\epsilon(\cdot,\boldsymbol{y}_\epsilon,\boldsymbol{z}_\epsilon)-v^s_\epsilon(\cdot,\boldsymbol{y}_\epsilon,\boldsymbol{z}_\epsilon). \tag{2.30}$$

It solves the scattering problem

$$\begin{cases}\Delta e_\epsilon(\cdot,\boldsymbol{y}_\epsilon,\boldsymbol{z}_\epsilon)+k^2e_\epsilon(\cdot,\boldsymbol{y}_\epsilon,\boldsymbol{z}_\epsilon)=0 \quad \text{in } \mathbb{R}^2\setminus\{\overline{D\cup D_\epsilon}\},\\ e_\epsilon(\cdot,\boldsymbol{y}_\epsilon,\boldsymbol{z}_\epsilon)=0 \quad \text{on } \partial D,\\ e_\epsilon(\cdot,\boldsymbol{y}_\epsilon,\boldsymbol{z}_\epsilon)=f_\epsilon(\cdot,\boldsymbol{y}_\epsilon,\boldsymbol{z}_\epsilon) \quad \text{on } \partial D_\epsilon,\\ e_\epsilon(\cdot,\boldsymbol{y}_\epsilon,\boldsymbol{z}_\epsilon) \text{ is radiating},\end{cases} \tag{2.31}$$

with $f_\epsilon(\cdot,\boldsymbol{y}_\epsilon,\boldsymbol{z}_\epsilon)=-u^s(\cdot,\boldsymbol{z}_\epsilon)-v^s_\epsilon(\cdot,\boldsymbol{y}_\epsilon,\boldsymbol{z}_\epsilon)$. We are now ready to prove our main result.

Theorem 2.4 (estimates on e_ϵ). *There exists a constant $C>0$, independent of ϵ, such that for small enough ϵ,*

$$\|e_\epsilon(\cdot,\boldsymbol{y}_\epsilon,\boldsymbol{z}_\epsilon)\|_{H^1(B)}\le C|\log\epsilon|^{-1}\epsilon^p\epsilon^{q/2}. \tag{2.32}$$

Proof. Consider the solution $u_\epsilon(\cdot,\boldsymbol{y}_\epsilon,\boldsymbol{z}_\epsilon)\in H^1_{\mathrm{loc}}(\mathbb{R}^2\setminus D_\epsilon)$ to

$$\begin{cases}\Delta u_\epsilon(\cdot,\boldsymbol{y}_\epsilon,\boldsymbol{z}_\epsilon)+k^2u_\epsilon(\cdot,\boldsymbol{y}_\epsilon,\boldsymbol{z}_\epsilon)=0 \quad \text{in } \mathbb{R}^2\setminus\overline{D_\epsilon},\\ u_\epsilon(\cdot,\boldsymbol{y}_\epsilon,\boldsymbol{z}_\epsilon)=f_\epsilon(\cdot,\boldsymbol{y}_\epsilon,\boldsymbol{z}_\epsilon) \quad \text{on } \partial D_\epsilon,\\ u_\epsilon(\cdot,\boldsymbol{y}_\epsilon,\boldsymbol{z}_\epsilon) \text{ is radiating}.\end{cases} \tag{2.33}$$

Then, $w_\epsilon=e_\epsilon-u_\epsilon\in H^1_{\mathrm{loc}}(\mathbb{R}^2\setminus\{D\cup D_\epsilon\})$ satisfies

$$\begin{cases}\Delta w_\epsilon(\cdot,\boldsymbol{y}_\epsilon,\boldsymbol{z}_\epsilon)+k^2w_\epsilon(\cdot,\boldsymbol{y}_\epsilon,\boldsymbol{z}_\epsilon)=0 \quad \text{in } \mathbb{R}^2\setminus\{\overline{D\cup D_\epsilon}\},\\ w_\epsilon(\cdot,\boldsymbol{y}_\epsilon,\boldsymbol{z}_\epsilon)=-u_\epsilon(\cdot,\boldsymbol{y}_\epsilon,\boldsymbol{z}_\epsilon) \quad \text{on } \partial D,\\ w_\epsilon(\cdot,\boldsymbol{y}_\epsilon,\boldsymbol{z}_\epsilon)=0 \quad \text{on } \partial D_\epsilon,\\ w_\epsilon(\cdot,\boldsymbol{y}_\epsilon,\boldsymbol{z}_\epsilon) \text{ is radiating}.\end{cases} \tag{2.34}$$

Utilizing Theorem B.2, there exists a constant $C>0$, independent of ϵ, such that for small enough ϵ,

$$\|w_\epsilon(\cdot,\boldsymbol{y}_\epsilon,\boldsymbol{z}_\epsilon)\|_{H^1(B)}\le C\|u_\epsilon(\cdot,\boldsymbol{y}_\epsilon,\boldsymbol{z}_\epsilon)\|_{H^{1/2}(\partial D)}. \tag{2.35}$$

This yields

$$\|e_\epsilon(\cdot,\boldsymbol{y}_\epsilon,\boldsymbol{z}_\epsilon)\|_{H^1(B)}\le\|u_\epsilon(\cdot,\boldsymbol{y}_\epsilon,\boldsymbol{z}_\epsilon)\|_{H^1(B)}+C\|u_\epsilon(\cdot,\boldsymbol{y}_\epsilon,\boldsymbol{z}_\epsilon)\|_{H^{1/2}(\partial D)}. \tag{2.36}$$

We write $u_\epsilon(\cdot,\boldsymbol{y}_\epsilon,\boldsymbol{z}_\epsilon)=-\mathscr{S}_\epsilon S_\epsilon^{-1}f_\epsilon(\cdot,\boldsymbol{y}_\epsilon,\boldsymbol{z}_\epsilon)$ in B and $u_\epsilon(\cdot,\boldsymbol{y}_\epsilon,\boldsymbol{z}_\epsilon)=-T_\epsilon S_\epsilon^{-1}f_\epsilon(\cdot,\boldsymbol{y}_\epsilon,\boldsymbol{z}_\epsilon)$ on ∂D with $f_\epsilon(\cdot,\boldsymbol{y}_\epsilon,\boldsymbol{z}_\epsilon)=-u^s(\cdot,\boldsymbol{z}_\epsilon)-v^s_\epsilon(\cdot,\boldsymbol{y}_\epsilon,\boldsymbol{z}_\epsilon)$. Using the estimates for $\mathscr{S}_\epsilon$ and T_ϵ (see Lemma B.1) and applying Theorem A.3 to $f_\epsilon(\cdot,\boldsymbol{y}_\epsilon,\boldsymbol{z}_\epsilon)$ with $r=p/2+q/2$, we obtain, for small enough ϵ,

$$\|u_\epsilon(\cdot,\boldsymbol{y}_\epsilon,\boldsymbol{z}_\epsilon)\|_{H^1(B)}\le\|\mathscr{S}_\epsilon\|\,\|S_\epsilon^{-1}f_\epsilon(\cdot,\boldsymbol{y}_\epsilon,\boldsymbol{z}_\epsilon)\|_{H^{-1/2}(\partial D_\epsilon)}\le C|\log\epsilon|^{-1}\epsilon^p\epsilon^{q/2} \tag{2.37}$$

and

$$\|u_\epsilon(\cdot,\boldsymbol{y}_\epsilon,\boldsymbol{z}_\epsilon)\|_{H^{1/2}(\partial D)} \le \|T_\epsilon\|\,\|S_\epsilon^{-1} f_\epsilon(\cdot,\boldsymbol{y}_\epsilon,\boldsymbol{z}_\epsilon)\|_{H^{-1/2}(\partial D_\epsilon)} \le C|\log\epsilon|^{-1}\epsilon^p\epsilon^{q/2}, \tag{2.38}$$

with a constant C independent of ϵ. ∎

We summarize our asymptotic results in Table 1. We note, in particular, that the error, as expressed in (2.30), is $\mathcal{O}(|\log\epsilon|^{-1}\epsilon^p\epsilon^{q/2})$ in the $H^1(B)$-norm, according to Theorem 2.4. This error comes from the scattering sequence $\phi(\cdot,\boldsymbol{z}_\epsilon)\to D\to u^s\to D_\epsilon\to e_\epsilon\to e_\epsilon|_B$, which generates a field smaller than the sequence $\phi(\cdot,\boldsymbol{z}_\epsilon)\to D_\epsilon\to v_\epsilon^i\to D\to v_\epsilon^s\to v_\epsilon^s|_B$. We also illustrate our asymptotic model in Figure 3.

Moving forward, we will utilize approximations for $v_\epsilon^i(\cdot,\boldsymbol{y}_\epsilon,\boldsymbol{z}_\epsilon)$ and $v_\epsilon^s(\cdot,\boldsymbol{y}_\epsilon,\boldsymbol{z}_\epsilon)$, based on the asymptotics of [9]. For instance, $v_\epsilon^i(\cdot,\boldsymbol{y}_\epsilon,\boldsymbol{z}_\epsilon)$ can be approximated by the field

$$\tilde v_\epsilon^i(\cdot,\boldsymbol{y}_\epsilon,\boldsymbol{z}_\epsilon) = \mu_\epsilon(\boldsymbol{y}_\epsilon,\boldsymbol{z}_\epsilon)\phi(\cdot,\boldsymbol{y}_\epsilon) \tag{2.39}$$

transmitted by a point source located at $\boldsymbol{y}_\epsilon$ with amplitude

$$\mu_\epsilon(\boldsymbol{y}_\epsilon,\boldsymbol{z}_\epsilon) = -H_0^{(1)}(k|\boldsymbol{y}_\epsilon-\boldsymbol{z}_\epsilon|)/H_0^{(1)}(2\pi\epsilon). \tag{2.40}$$

(This is why we use the superscript "i" in v_ϵ^i—it is an incident field for D.) Similarly, let $\tilde v_\epsilon^s(\cdot,\boldsymbol{y}_\epsilon,\boldsymbol{z}_\epsilon)$ be the solution to (2.7) with $v_\epsilon^i(\cdot,\boldsymbol{y}_\epsilon,\boldsymbol{z}_\epsilon)$ replaced by $\tilde v_\epsilon^i(\cdot,\boldsymbol{y}_\epsilon,\boldsymbol{z}_\epsilon)$. Then,

$$\tilde v_\epsilon^s(\cdot,\boldsymbol{y}_\epsilon,\boldsymbol{z}_\epsilon) = \mu_\epsilon(\boldsymbol{y}_\epsilon,\boldsymbol{z}_\epsilon)u^s(\cdot,\boldsymbol{y}_\epsilon), \tag{2.41}$$

where $u^s(\cdot,\boldsymbol{y}_\epsilon)$ is the solution to the scattering problem (2.5) for the incident wave $\phi(\cdot,\boldsymbol{y}_\epsilon)$.

Let $\tilde e_\epsilon(\cdot,\boldsymbol{y}_\epsilon,\boldsymbol{z}_\epsilon)\in H^1_{\rm loc}(\mathbb{R}^2\setminus\{D\cup\{\boldsymbol{y}_\epsilon\}\})$ be the error

$$\tilde e_\epsilon(\cdot,\boldsymbol{y}_\epsilon,\boldsymbol{z}_\epsilon) = w_\epsilon^s(\cdot,\boldsymbol{y}_\epsilon,\boldsymbol{z}_\epsilon) - u^s(\cdot,\boldsymbol{z}_\epsilon) - \tilde v_\epsilon^i(\cdot,\boldsymbol{y}_\epsilon,\boldsymbol{z}_\epsilon) - \tilde v_\epsilon^s(\cdot,\boldsymbol{y}_\epsilon,\boldsymbol{z}_\epsilon). \tag{2.42}$$

It solves the scattering problem

$$\begin{cases} \Delta\tilde e_\epsilon(\cdot,\boldsymbol{y}_\epsilon,\boldsymbol{z}_\epsilon) + k^2\tilde e_\epsilon(\cdot,\boldsymbol{y}_\epsilon,\boldsymbol{z}_\epsilon) = 0 \quad \text{in } \mathbb{R}^2\setminus\{\overline{D}\cup\{\boldsymbol{y}_\epsilon\}\},\\ \tilde e_\epsilon(\cdot,\boldsymbol{y}_\epsilon,\boldsymbol{z}_\epsilon) = 0 \quad \text{on } \partial D,\\ \tilde e_\epsilon(\cdot,\boldsymbol{y}_\epsilon,\boldsymbol{z}_\epsilon) = \tilde f_\epsilon(\cdot,\boldsymbol{y}_\epsilon,\boldsymbol{z}_\epsilon) \quad \text{on } \partial D_\epsilon,\\ e_\epsilon(\cdot,\boldsymbol{y}_\epsilon,\boldsymbol{z}_\epsilon) \text{ is radiating}, \end{cases} \tag{2.43}$$

with $\tilde f_\epsilon(\cdot,\boldsymbol{y}_\epsilon,\boldsymbol{z}_\epsilon) = \phi(\cdot,\boldsymbol{z}_\epsilon) - u^s(\cdot,\boldsymbol{z}_\epsilon) - \tilde v_\epsilon^i(\cdot,\boldsymbol{y}_\epsilon,\boldsymbol{z}_\epsilon) - \tilde v_\epsilon^s(\cdot,\boldsymbol{y}_\epsilon,\boldsymbol{z}_\epsilon)$. We obtain the following theorem from Theorem 2.4 and the formulas (2.39) and (2.41) for $\tilde v_\epsilon^i$ and $\tilde v_\epsilon^s$.

Table 1

The amplitude of the scattered fields u^s, v_ϵ^i, v_ϵ^s, and e_ϵ, described by (2.5)–(2.7) and (2.30), depends on ϵ. The estimates are proved in Lemmas 2.1, 2.2, and 2.3 and Theorem 2.4.

Scattering sequence	$H^1(B)$-norm
$\phi(\cdot,\boldsymbol{z}_\epsilon) \underset{\text{incident}}{\longrightarrow} D \underset{\text{scattering}}{\longrightarrow} u^s \underset{\text{evaluation}}{\longrightarrow} u^s\|_B$	$\mathcal{O}(\epsilon^{q/2})$
$\phi(\cdot,\boldsymbol{z}_\epsilon) \underset{\text{incident}}{\longrightarrow} D_\epsilon \underset{\text{scattering}}{\longrightarrow} v_\epsilon^i \underset{\text{evaluation}}{\longrightarrow} v_\epsilon^i\|_B$	$\mathcal{O}(\|\log\epsilon\|^{-1}\epsilon^{p/2}\epsilon^{q/2})$
$\phi(\cdot,\boldsymbol{z}_\epsilon) \underset{\text{incident}}{\longrightarrow} D_\epsilon \underset{\text{scattering}}{\longrightarrow} v_\epsilon^i \underset{\text{incident}}{\longrightarrow} D \underset{\text{scattering}}{\longrightarrow} v_\epsilon^s \underset{\text{evaluation}}{\longrightarrow} v_\epsilon^s\|_B$	$\mathcal{O}(\|\log\epsilon\|^{-1}\epsilon^{p/2}\epsilon^{q/2})$
$\phi(\cdot,\boldsymbol{z}_\epsilon) \underset{\text{incident}}{\longrightarrow} D \underset{\text{scattering}}{\longrightarrow} u^s \underset{\text{incident}}{\longrightarrow} D_\epsilon \underset{\text{scattering}}{\longrightarrow} e_\epsilon \underset{\text{evaluation}}{\longrightarrow} e_\epsilon\|_B$	$\mathcal{O}(\|\log\epsilon\|^{-1}\epsilon^{p}\epsilon^{q/2})$

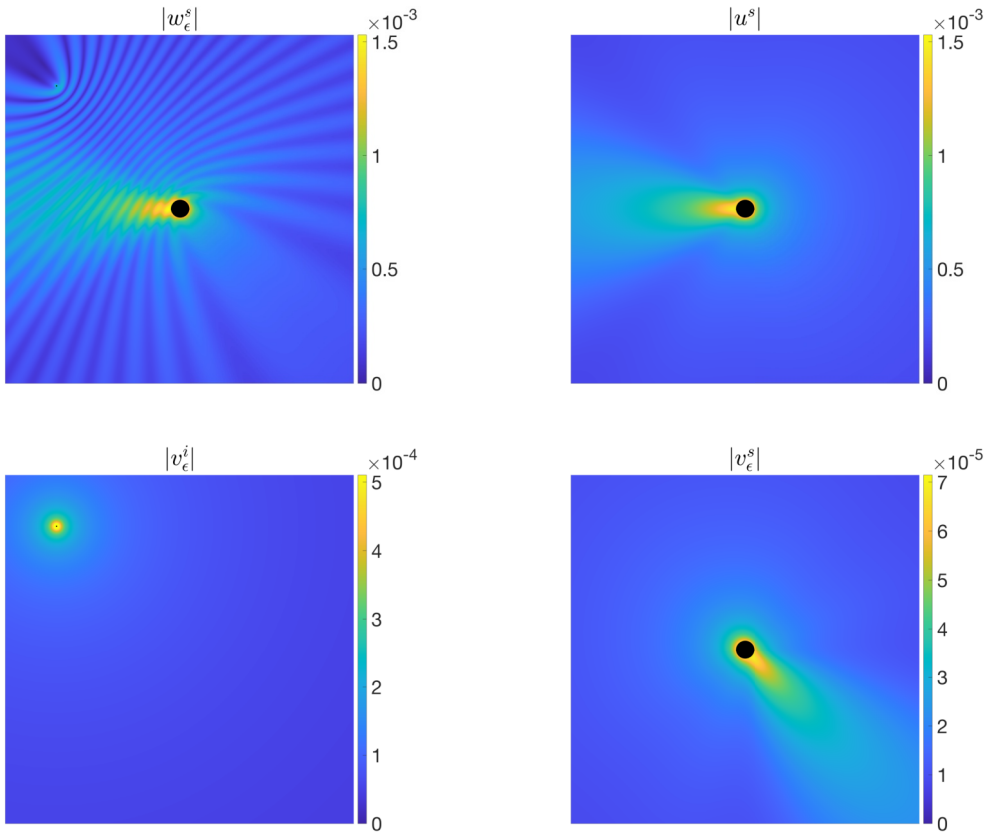

Figure 3. *The scattered field w_ϵ^s (top left) can be approximated with an error $\mathcal{O}(|\log\epsilon|^{-1}\epsilon^p\epsilon^{q/2})$ by the sum of three terms: u^s (top right), v_ϵ^i (bottom left), and v_ϵ^s (bottom right). The relevant signal for the LSM is stored in the total field $v_\epsilon = v_\epsilon^i + v_\epsilon^s$, which satisfies a modified Helmholtz–Kirchhoff identity (section 3).*

Theorem 2.5 (estimates on $\tilde{e}_\epsilon$). *There exists a constant $C > 0$, independent of ϵ, such that for small enough ϵ,*

$$\|\tilde{e}_\epsilon(\cdot, \boldsymbol{y}_\epsilon, \boldsymbol{z}_\epsilon)\|_{H^1(B)} \leq C(|\log\epsilon|^{-1}\epsilon^p\epsilon^{q/2} + \epsilon^{p/2}\epsilon^{q/2}\epsilon^2). \tag{2.44}$$

Proof. We combine (2.30) with (2.42) to write

$$\tilde{e}_\epsilon(\cdot, \boldsymbol{y}_\epsilon, \boldsymbol{z}_\epsilon) = e_\epsilon(\cdot, \boldsymbol{y}_\epsilon, \boldsymbol{z}_\epsilon) + \tilde{v}_\epsilon^i(\cdot, \boldsymbol{y}_\epsilon, \boldsymbol{z}_\epsilon) - v_\epsilon^i(\cdot, \boldsymbol{y}_\epsilon, \boldsymbol{z}_\epsilon) + \tilde{v}_\epsilon^s(\cdot, \boldsymbol{y}_\epsilon, \boldsymbol{z}_\epsilon) - v_\epsilon^s(\cdot, \boldsymbol{y}_\epsilon, \boldsymbol{z}_\epsilon). \tag{2.45}$$

Let us define $e_\epsilon^i = \tilde{v}_\epsilon^i - v_\epsilon^i$ and $e_\epsilon^s = \tilde{v}_\epsilon^s - v_\epsilon^s$. These solve the scattering problems

$$\begin{cases} \Delta e_\epsilon^i(\cdot, \boldsymbol{y}_\epsilon, \boldsymbol{z}_\epsilon) + k^2 e_\epsilon^i(\cdot, \boldsymbol{y}_\epsilon, \boldsymbol{z}_\epsilon) = 0 \quad \text{in } \mathbb{R}^2 \setminus \overline{D_\epsilon}, \\ e_\epsilon^i(\cdot, \boldsymbol{y}_\epsilon, \boldsymbol{z}_\epsilon) = -(\phi(\boldsymbol{y}_\epsilon, \boldsymbol{z}_\epsilon) - \phi(\cdot, \boldsymbol{z}_\epsilon)) \quad \text{on } \partial D_\epsilon, \\ e_\epsilon^i(\cdot, \boldsymbol{y}_\epsilon, \boldsymbol{z}_\epsilon) \text{ is radiating}, \end{cases} \tag{2.46}$$

and

$$\text{(2.47)}\qquad \begin{cases} \Delta e^s_\epsilon(\cdot,\boldsymbol{y}_\epsilon,\boldsymbol{z}_\epsilon)+k^2 e^s_\epsilon(\cdot,\boldsymbol{y}_\epsilon,\boldsymbol{z}_\epsilon)=0 \quad \text{in } \mathbb{R}^2\setminus\overline{D},\\ e^s_\epsilon(\cdot,\boldsymbol{y}_\epsilon,\boldsymbol{z}_\epsilon)=-e^i_\epsilon(\cdot,\boldsymbol{y}_\epsilon,\boldsymbol{z}_\epsilon) \quad \text{on } \partial D,\\ e^s_\epsilon(\cdot,\boldsymbol{y}_\epsilon,\boldsymbol{z}_\epsilon) \text{ is radiating.} \end{cases}$$

We note that, using the notations of Lemma 2.2,

$$\text{(2.48)}\qquad e^i_\epsilon(\boldsymbol{x},\boldsymbol{y}_\epsilon,\boldsymbol{z}_\epsilon)=-\frac{i}{4}\frac{H_0^{(1)}(k|\boldsymbol{y}_\epsilon-\boldsymbol{z}_\epsilon|)(1-J_0(2\pi\epsilon))}{H_0^{(1)}(2\pi\epsilon)}H_0^{(1)}(k|\boldsymbol{x}-\boldsymbol{y}_\epsilon|)$$
$$-\frac{i}{4}\sum_{|n|\neq 0}\frac{H_n^{(1)}(k|\boldsymbol{y}_\epsilon-\boldsymbol{z}_\epsilon|)J_n(2\pi\epsilon)}{H_n^{(1)}(2\pi\epsilon)}e^{-in(\mu_\epsilon+\pi)}H_n^{(1)}(k|\boldsymbol{x}-\boldsymbol{y}_\epsilon|)e^{in\theta}.$$

We write $e^i_\epsilon(\cdot,\boldsymbol{y}_\epsilon,\boldsymbol{z}_\epsilon)=-\mathscr{S}_\epsilon S_\epsilon^{-1}f(\cdot,\boldsymbol{y}_\epsilon,\boldsymbol{z}_\epsilon)$ in B and $e^i_\epsilon(\cdot,\boldsymbol{y}_\epsilon,\boldsymbol{z}_\epsilon)=-T_\epsilon S_\epsilon^{-1}f(\cdot,\boldsymbol{y}_\epsilon,\boldsymbol{z}_\epsilon)$ on ∂D with $f(\cdot,\boldsymbol{y}_\epsilon,\boldsymbol{z}_\epsilon)=-(\phi(\boldsymbol{y}_\epsilon,\boldsymbol{z}_\epsilon)-\phi(\cdot,\boldsymbol{z}_\epsilon))$. Applying Lemma B.1 to $f(\cdot,\boldsymbol{y}_\epsilon,\boldsymbol{z}_\epsilon)$ with $r=q/2$, we obtain, for small enough ϵ,

$$\text{(2.49)}\qquad \|e^i_\epsilon(\cdot,\boldsymbol{y}_\epsilon,\boldsymbol{z}_\epsilon)\|_{H^{1/2}(\partial D)}=\|T_\epsilon S_\epsilon^{-1}f_\epsilon(\cdot,\boldsymbol{y}_\epsilon,\boldsymbol{z}_\epsilon)\|_{H^{1/2}(\partial D)}\le C\epsilon^{p/2}\epsilon^{q/2}\epsilon^2$$

and

$$\text{(2.50)}\qquad \|e^i_\epsilon(\cdot,\boldsymbol{y}_\epsilon,\boldsymbol{z}_\epsilon)\|_{H^1(B)}=\|\mathscr{S}_\epsilon S_\epsilon^{-1}f_\epsilon(\cdot,\boldsymbol{y}_\epsilon,\boldsymbol{z}_\epsilon)\|_{H^1(B)}\le C\epsilon^{p/2}\epsilon^{q/2}\epsilon^2$$

with a constant C independent of ϵ. We conclude by noting that

$$\text{(2.51)}\qquad \|e^s_\epsilon(\cdot,\boldsymbol{y}_\epsilon,\boldsymbol{z}_\epsilon)\|_{H^1(B)}\le C\|e^i_\epsilon(\cdot,\boldsymbol{y}_\epsilon,\boldsymbol{z}_\epsilon)\|_{H^{1/2}(\partial D)}$$

and using the triangle inequality. ∎

In the proof of Theorem 2.5, we showed that approximating v^i_ϵ by $\tilde{v}^i_\epsilon$ yields an error $\mathcal{O}(\epsilon^2)$ when $p=q=0$. This is sharper than the error $\mathcal{O}(|\log\epsilon|^{-1}\epsilon)$ proved in [9, Thm. 1].

3. A modified Helmholtz–Kirchhoff identity. In this section, we will establish that the total field $\tilde{v}_\epsilon=\tilde{v}^i_\epsilon+\tilde{v}^s_\epsilon$ satisfies a *modified* Helmholtz–Kirchhoff identity. Consequently, the information is encapsulated in $\tilde{v}_\epsilon$. However, the practical challenge lies in having access only to measurements of $w^s_\epsilon=u^s+\tilde{v}_\epsilon+\tilde{e}_\epsilon$. We first outline the process of extracting $\tilde{v}_\epsilon$.

Let Σ_ϵ be the circle of radius $\lambda\epsilon^{-p}$ centered at the origin and let $\langle\cdot\rangle$ denote the average with respect to $\boldsymbol{y}_\epsilon\in\Sigma_\epsilon$, e.g.,

$$\text{(3.1)}\qquad \langle w^s_\epsilon\rangle(\boldsymbol{x},\boldsymbol{z}_\epsilon)=\frac{1}{|\Sigma_\epsilon|}\int_{\Sigma_\epsilon}w^s_\epsilon(\boldsymbol{x},\boldsymbol{y}_\epsilon,\boldsymbol{z}_\epsilon)ds(\boldsymbol{y}_\epsilon).$$

Since $u^s(\cdot,\boldsymbol{z}_\epsilon)$ does not depend on $\boldsymbol{y}_\epsilon\in\Sigma_\epsilon$, we note that, for any $\boldsymbol{x}\in B$,

$$\text{(3.2)}\qquad w^s_\epsilon(\boldsymbol{x},\boldsymbol{y}_\epsilon,\boldsymbol{z}_\epsilon)-\langle w^s_\epsilon\rangle(\boldsymbol{x},\boldsymbol{z}_\epsilon)=\tilde{v}_\epsilon(\boldsymbol{x},\boldsymbol{y}_\epsilon,\boldsymbol{z}_\epsilon)-\langle\tilde{v}_\epsilon\rangle(\boldsymbol{x},\boldsymbol{z}_\epsilon)+\tilde{e}_\epsilon(\boldsymbol{x},\boldsymbol{y}_\epsilon,\boldsymbol{z}_\epsilon)-\langle\tilde{e}_\epsilon\rangle(\boldsymbol{x},\boldsymbol{z}_\epsilon).$$

We are going to show that the $\boldsymbol{y}_\epsilon$-average of $\tilde{v}_\epsilon$ is small in comparison to $\tilde{v}_\epsilon$ (Theorem 3.1). Therefore, removing the $\boldsymbol{y}_\epsilon$-average of w^s_ϵ from w^s_ϵ is a simple way of accessing $\tilde{v}_\epsilon$, as the other three terms in the right-hand side of (3.2) are negligible.

Theorem 3.1 (norm of $\tilde{v}_\epsilon$ and $\langle\tilde{v}_\epsilon\rangle$). *There exists a constant $C>0$, independent of ϵ, such that for small enough ϵ,*

$$\|\tilde{v}_\epsilon(\cdot,\boldsymbol{y}_\epsilon,\boldsymbol{z}_\epsilon)\|_{H^1(B)} \le C|\log\epsilon|^{-1}\epsilon^{p/2}\epsilon^{q/2} \tag{3.3}$$

and

$$\|\langle\tilde{v}_\epsilon\rangle(\cdot,\boldsymbol{z}_\epsilon)\|_{H^1(B)} \le C|\log\epsilon|^{-1}\epsilon^{p}\epsilon^{q/2}. \tag{3.4}$$

Proof. The first estimate can be obtained via those on $v^i_\epsilon(\cdot,\boldsymbol{y}_\epsilon,\boldsymbol{z}_\epsilon)$ (Theorem 2.2) and $v^s_\epsilon(\cdot,\boldsymbol{y}_\epsilon,\boldsymbol{z}_\epsilon)$ (Lemma 2.3), or via Lemma C.8. For the second estimate, we first note that the amplitude of $\langle\tilde{v}^i_\epsilon\rangle(\cdot,\boldsymbol{z}_\epsilon)$ can be estimated using Lemma C.8. To conclude, we observe that $\langle\tilde{v}^s_\epsilon\rangle(\cdot,\boldsymbol{z}_\epsilon)$ is a scattered field for the incident wave $\langle\tilde{v}^i_\epsilon\rangle(\cdot,\boldsymbol{z}_\epsilon)$. ∎

For any $\boldsymbol{x}'\in\mathbb{R}^2\setminus\overline{D}$, we recall that $u^s(\cdot,\boldsymbol{x}')$ denotes the solution to (2.5) for the incident wave $\phi(\cdot,\boldsymbol{x}')$. In our previous work, we utilize the fact that $u^s(\cdot,\boldsymbol{x}')$ and the associated total field $u(\boldsymbol{x},\boldsymbol{x}')=\phi(\cdot,\boldsymbol{x}')+u^s(\cdot,\boldsymbol{x}')$ verify the following Helmholtz–Kirchhoff identity:

$$u^s(\boldsymbol{x},\boldsymbol{x}')-\overline{u^s(\boldsymbol{x},\boldsymbol{x}')}=2ik\int_\Sigma \overline{u(\boldsymbol{x},\boldsymbol{z})}u(\boldsymbol{x}',\boldsymbol{z})ds(\boldsymbol{z})-\left[\phi(\boldsymbol{x},\boldsymbol{x}')-\overline{\phi(\boldsymbol{x},\boldsymbol{x}')}\right]. \tag{3.5}$$

This motivated the setup of Figure 4 (left) and the introduction of the cross-correlation matrix (1.2). Indeed, in that setup, we assumed that the $J>0$ measurement points $\boldsymbol{x}_j$ are located in some bounded volume $B\subset\mathbb{R}^2\setminus\overline{D}$. We also assumed that there exists a surface Σ that encloses B and D, and that there are $L>0$ point sources $\boldsymbol{z}_\ell$ randomly distributed on Σ. These sources can transmit a unit-amplitude time-harmonic signal, one by one, so that it is possible to measure the total fields $u(\boldsymbol{x}_j,\boldsymbol{z}_\ell)$. Moreover, it is possible to compute $\phi(\boldsymbol{x}_j,\boldsymbol{x}_m)$, so we can evaluate the cross-correlation matrix (1.2). This matrix corresponds to the discretization of the right-hand side of (3.5) at points $\boldsymbol{z}_\ell$ with uniform weights and evaluated at $\boldsymbol{x}_j$ and $\boldsymbol{x}_m$, i.e.,

$$C_{jm}\approx 2ik\int_\Sigma \overline{u(\boldsymbol{x}_j,\boldsymbol{z})}u(\boldsymbol{x}_m,\boldsymbol{z})ds(\boldsymbol{z})-\left[\phi(\boldsymbol{x}_j,\boldsymbol{x}_m)-\overline{\phi(\boldsymbol{x}_j,\boldsymbol{x}_m)}\right]. \tag{3.6}$$

The quadrature error associated with (3.6) is $\mathcal{O}(1/\sqrt{L})$, in general. However, if the $\boldsymbol{z}_\ell$'s correspond to a β-perturbed trapezoidal rule, i.e., $\boldsymbol{z}_\ell=2\pi(\ell-1+\beta_\ell)/L$ with $|\beta_\ell|\le\beta<1/2$ for all $1\le\ell\le L$, then the error improves to $\mathcal{O}(1/L^{\nu-4\beta})$ whenever the integrand has $\nu>4\beta+1/2$ derivatives [5, Thm. 1]. (For details about computations with trigonometric interpolants, we refer the reader to [24, 31, 33].)

We show, now, that the total field $\tilde{v}_\epsilon=\tilde{v}^i_\epsilon+\tilde{v}^s_\epsilon$ satisfies a *modified* Helmholtz–Kirchhoff identity, which justifies the setup of Figure 4 (right).

Theorem 3.2 (modified Helmholtz–Kirchhoff identity). *For any point $\boldsymbol{x}$ and $\boldsymbol{x}'$ in B, and small enough ϵ,*

$$\begin{aligned}u^s(\boldsymbol{x},\boldsymbol{x}')-\overline{u^s(\boldsymbol{x},\boldsymbol{x}')}=2ik\sigma_\epsilon\int_{\Sigma_\epsilon}\overline{\tilde{v}_\epsilon(\boldsymbol{x},\boldsymbol{y}_\epsilon,\boldsymbol{z}_\epsilon)}\tilde{v}_\epsilon(\boldsymbol{x}',\boldsymbol{y}_\epsilon,\boldsymbol{z}_\epsilon)ds(\boldsymbol{y}_\epsilon)\left[1+\mathcal{O}(\epsilon^{q-p})\right]\\ -\left[\phi(\boldsymbol{x},\boldsymbol{x}')-\overline{\phi(\boldsymbol{x},\boldsymbol{x}')}\right],\end{aligned} \tag{3.7}$$

where the scaling factor σ_ϵ reads

$$\sigma_\epsilon=\pi^2|H_0^{(1)}(2\pi\epsilon)|^2\epsilon^{-q}. \tag{3.8}$$

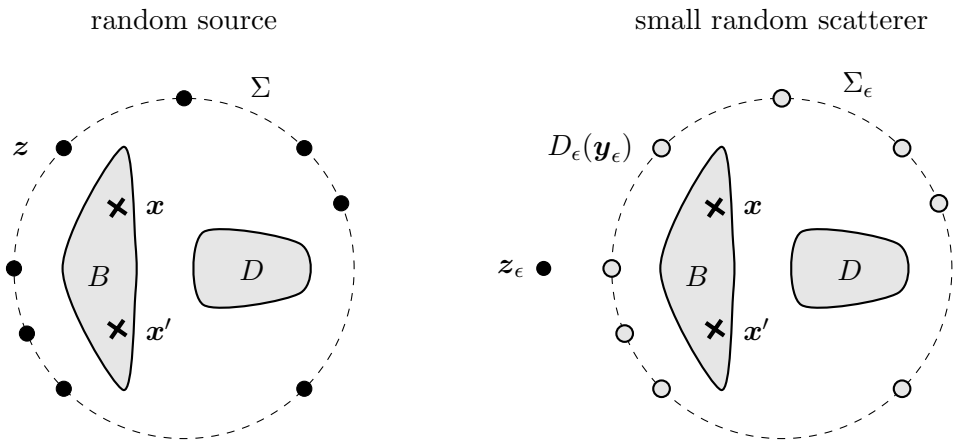

Figure 4. *In passive imaging with a random source (left), the defect D is illuminated by an uncontrolled, random source located at points $\boldsymbol{z}$, which we assume to be distributed on a surface Σ that encloses the defect. The medium's response is recorded at points $\boldsymbol{x}$ and $\boldsymbol{x}'$, contained in some measurement volume B. In passive imaging with a small random scatterer (right), the defect is illuminated by a single controlled point source located at $\boldsymbol{z}_\epsilon$. The incident field is scattered by a small random scatterer $D_\epsilon(\boldsymbol{y}_\epsilon)$ whose center $\boldsymbol{y}_\epsilon$ is located on Σ_ϵ, creating a secondary, random source. The medium's response is recorded in some volume B.*

Proof. Recall that

$$\tilde{v}_\epsilon^i(\boldsymbol{x},\boldsymbol{y}_\epsilon,\boldsymbol{z}_\epsilon)=\mu_\epsilon(\boldsymbol{y}_\epsilon,\boldsymbol{z}_\epsilon)\phi(\boldsymbol{x},\boldsymbol{y}_\epsilon) \quad \text{and} \quad \tilde{v}_\epsilon^s(\boldsymbol{x},\boldsymbol{y}_\epsilon,\boldsymbol{z}_\epsilon)=\mu_\epsilon(\boldsymbol{y}_\epsilon,\boldsymbol{z}_\epsilon)u^s(\boldsymbol{x},\boldsymbol{y}_\epsilon). \tag{3.9}$$

Therefore,

$$u^s(\boldsymbol{x},\boldsymbol{y}_\epsilon)=\mu_\epsilon(\boldsymbol{y}_\epsilon,\boldsymbol{z}_\epsilon)^{-1}\tilde{v}_\epsilon^s(\boldsymbol{x},\boldsymbol{y}_\epsilon,\boldsymbol{z}_\epsilon) \tag{3.10}$$

satisfies the standard Helmholtz–Kirchhoff identity

$$u^s(\boldsymbol{x},\boldsymbol{x}')-\overline{u^s(\boldsymbol{x},\boldsymbol{x}')}=2ik\int_{\Sigma_\epsilon}\overline{u(\boldsymbol{x},\boldsymbol{y}_\epsilon)}u(\boldsymbol{x}',\boldsymbol{y}_\epsilon)ds(\boldsymbol{y}_\epsilon)-\left[\phi(\boldsymbol{x},\boldsymbol{x}')-\overline{\phi(\boldsymbol{x},\boldsymbol{x}')}\right], \tag{3.11}$$

with total field

$$u(\boldsymbol{x},\boldsymbol{y}_\epsilon)=\phi(\boldsymbol{x},\boldsymbol{y}_\epsilon)+u^s(\boldsymbol{x},\boldsymbol{y}_\epsilon)=\mu_\epsilon(\boldsymbol{y}_\epsilon,\boldsymbol{z}_\epsilon)^{-1}\tilde{v}_\epsilon(\boldsymbol{x},\boldsymbol{y}_\epsilon,\boldsymbol{z}_\epsilon). \tag{3.12}$$

We can rewrite the integral as

$$2ik\int_{\Sigma_\epsilon}|\mu_\epsilon(\boldsymbol{y}_\epsilon,\boldsymbol{z}_\epsilon)^{-1}|^2\,\overline{\tilde{v}_\epsilon(\boldsymbol{x},\boldsymbol{y}_\epsilon,\boldsymbol{z}_\epsilon)}\tilde{v}_\epsilon(\boldsymbol{x}',\boldsymbol{y}_\epsilon,\boldsymbol{z}_\epsilon)ds(\boldsymbol{y}_\epsilon). \tag{3.13}$$

We conclude by using Lemma C.9. ∎

Our modified Helmholtz–Kirchhoff identity in Theorem 3.2 justifies the introduction of the *modified* cross-correlation matrix,

$$\widetilde{C}_{jm}=\frac{2ik|\Sigma_\epsilon|\sigma_\epsilon}{L}\sum_{\ell=1}^{L}\overline{\tilde{v}_\epsilon(\boldsymbol{x}_j,\boldsymbol{y}_\epsilon^\ell,\boldsymbol{z}_\epsilon)}\tilde{v}_\epsilon(\boldsymbol{x}_m,\boldsymbol{y}_\epsilon^\ell,\boldsymbol{z}_\epsilon)-\left[\phi(\boldsymbol{x}_j,\boldsymbol{x}_m)-\overline{\phi(\boldsymbol{x}_j,\boldsymbol{x}_m)}\right], \tag{3.14}$$

whose accuracy and robustness we demonstrate next in a series of numerical experiments.

4. Numerical experiments. The solution to the inverse acoustic scattering problem consists of two steps. First, the modified cross-correlation matrix (3.14) is filled out in the data acquisition step (direct problem). This entails solving (2.2) for L different positions $\boldsymbol{y}_\epsilon^\ell$ of the small scatterer and evaluating the solution at J points $\boldsymbol{x}_j$ (for a given $\boldsymbol{z}_\epsilon$). This yields a $J \times L$ near-field matrix N with entries $N_{j\ell} = w_\epsilon^s(\boldsymbol{x}_j, \boldsymbol{y}_\epsilon^\ell, \boldsymbol{z}_\epsilon)$. We then remove its column-average, generating a $J \times L$ matrix $\widetilde{N}$ with entries $\widetilde{N}_{j\ell} \approx \tilde{v}_\epsilon(\boldsymbol{x}_j, \boldsymbol{y}_\epsilon^\ell, \boldsymbol{z}_\epsilon)$. This allows us to assemble the $J \times J$ matrix (3.14). Second, we probe the medium by solving the system $\widetilde{C} g_{\boldsymbol{s}} = \phi_{\boldsymbol{s}}$, for several sampling points $\boldsymbol{s} \in \mathbb{R}^2$, in the data processing step (inverse problem). The right-hand side reads $(\phi_{\boldsymbol{s}})_j = \phi(\boldsymbol{x}_j, \boldsymbol{s})$, $1 \le j \le J$. The boundary ∂D of the unknown defect D coincides with those points $\boldsymbol{s}$ for which $\|g_{\boldsymbol{s}}\|_2$ is large [18, Thm. 4.3].

Solving the direct problem. Our MATLAB implementation leverages the capabilities of gypsilab, an open-source toolbox designed for efficient boundary element computations [2]. The approach adopted employs the combined boundary integral formulation for the exterior Dirichlet problem (2.2), allowing for the computation of weakly and strongly singular and near-singular integrals through the methods delineated in [25, 26]. It is preferable to employ a combined integral approach, as it is coercive for large wavenumbers [30]. We utilize up to 100 points to discretize the boundary and aim for four-digit accuracy.

Solving the inverse problem. To simulate noisy measurements, we add some random noise with amplitude δ to the near-field matrix N, before constructing $\widetilde{C}$. This yields a noisy matrix $\widetilde{C}_\delta$. To solve $\widetilde{C}_\delta g_{\boldsymbol{s}} = \phi_{\boldsymbol{s}}$, we compute the SVD of the matrix $\widetilde{C}_\delta$, $\widetilde{C}_\delta = \widetilde{U}_\delta \widetilde{S}_\delta \widetilde{V}_\delta^*$, and apply Tikhonov regularization with parameter $\alpha > 0$. To choose α, we use Morozov's discrepancy principle. For details, we refer the reader to [18, sect. 5].

Full-aperture measurements. We consider an ellipse and a kite of size $\lambda/2$ centered at $-2\lambda - 2\lambda i$ and $2\lambda + 2\lambda i$ for the wavenumber $k = 2\pi$ (wavelength $\lambda = 1$). The ellipse has axes $a = 1.5$ and $b = 1$, while the kite is that of [13, sect. 3.6]. We take $\epsilon = 10^{-2}$, $p = 1$, $q = 2$, and $\theta_z = \pi$ for the asymptotic model, which yields $\boldsymbol{z}_\epsilon = -10000$. (We will keep all parameters listed thus far unchanged throughout all experiments.) For the LSM, we take $J = 120$ equispaced sensors on the circle of radius $5\lambda = 5$,

$$\boldsymbol{x}_j = 5e^{i\theta_x^j}, \quad \theta_x^j = \frac{2\pi}{J}(j-1), \quad 1 \le j \le J, \tag{4.1}$$

and $L = 150$ different positions of a single small scatterer on the circle of radius $\lambda\epsilon^{-p} = 100$,

$$\boldsymbol{y}_\epsilon^\ell = 100e^{i\theta_y^\ell}, \quad \theta_y^\ell = \frac{2\pi}{L}(\ell - 1 + \beta_\ell), \quad 1 \le \ell \le L, \tag{4.2}$$

where the β_ℓ's are independent and identically distributed with the uniform distribution over $(0, 0.1)$. This is a (slightly) perturbed equispaced grid, with the corresponding quadrature in (3.14) serving as an accurate approximation of the integral within (3.7) (see also the comments preceding Theorem 3.2). Finally, we add some multiplicative noise with amplitude 5×10^{-3} to the near-field measurements[4] and probe the medium on a 100×100 uniform grid on $[-6\lambda, 6\lambda] \times [-6\lambda, 6\lambda]$. The results are shown in Figures 5 and 6 for the ellipse and the kite. In

[4] In theory, to ensure the preservation of the signal encapsulated in $\tilde{v}_\epsilon$, the noise level must align, up to a logarithmic factor, with the approximation error $\mathcal{O}(\epsilon^p \epsilon^{q/2}) = 10^{-4}$ described in Theorem 2.4. However, in practice, we managed to obtain satisfactory reconstructions even with noise levels as high as 5×10^{-3}. This still presents a clear limitation, which we will partially address in the last experiment.

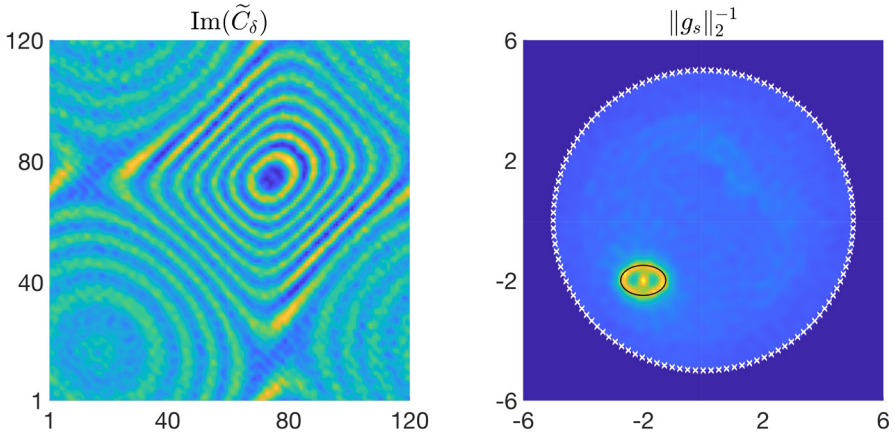

Figure 5. *The left picture displays the imaginary part of the modified cross-correlation matrix (3.14) and the right picture displays the indicator function (values outside of the disk of radius 5λ were zeroed out). The measurement points are represented by crosses, while the true boundary is depicted in a solid black line. Our sampling method, based on cross-correlations and a small random scatterer, successfully identified D.*

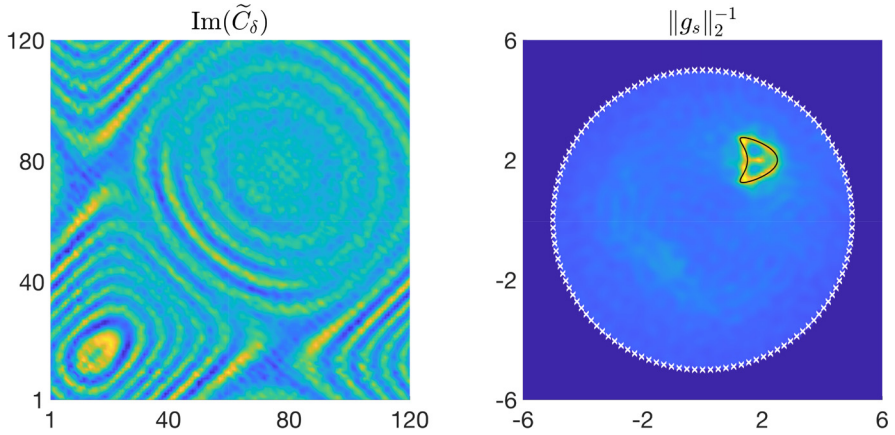

Figure 6. *In this experiment, too, the defect (a kite) is well identified by our method. This demonstrates that the LSM can be utilized in passive imaging with data generated by a small random scatterer. The setup in this figure is the same as in Figure 5.*

both cases, the defect is well identified by our novel LSM, based on cross-correlations and a small random scatterer. Our method can also handle several obstacles, as shown in Figure 7.

We now consider a less favorable but more realistic scenario where the positions of the single small scatterer move according to

$$\boldsymbol{y}_\epsilon^\ell = 100 e^{i\theta_y^\ell}, \quad 1 \le \ell \le L, \tag{4.3}$$

where the θ_y^ℓ's are independent and identically distributed with the uniform distribution over $(0, 2\pi)$. We present the results in Figure 8 for $J = 120$ sensors as described in (4.1), $L = 400$ realizations, and noise level 5×10^{-3}; these are not as good as previously. The reason for this is that the sum in (3.14) with the quadrature points as given by (4.3) is a rather poor approximation to the integral in (3.7), the quadrature error being $\mathcal{O}(1/\sqrt{L})$.

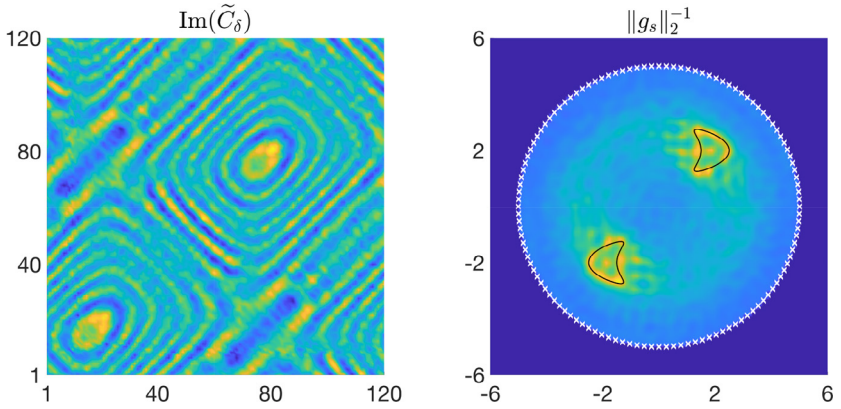

Figure 7. *Our method can handle several obstacles (here, two kites), as long as they are separated by a few wavelengths. The setup in this figure is the same as in Figure 5.*

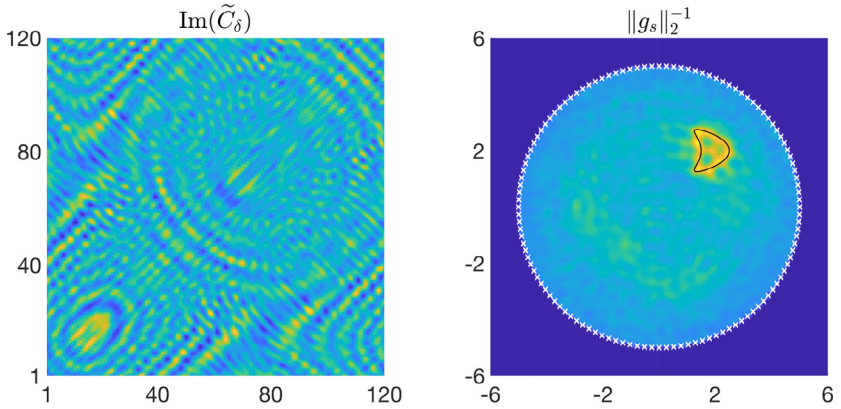

Figure 8. *When the small scatterer moves randomly around the obstacle according to (4.3), the quadrature error associated with our modified cross-correlation matrix is $\mathcal{O}(1/\sqrt{L})$. It is therefore necessary to increase the number of realizations L from 150 to 400 to obtain good numerical results. The entries of the matrix (on the left) are noisy approximations to those of Figure 6.*

Limited-aperture measurements. In this numerical experiment, we explore measurements with a restricted aperture, as analyzed in [4]. The outcomes are displayed in Figure 9 for $J = 120$ sensors, $L = 150$ different realizations of (4.2), and noise amplitude 5×10^{-3}. Although this configuration leads to much more challenging reconstructions, our approach based on the modified cross-correlation matrix (3.14) and a small random scatterer produces results comparable to those obtained using the cross-correlation matrix (1.2) and a random source (see [18, sect. 5]).

Several small scatterers. We now assume that there are $R > 1$ several small random scatterers around D. At each acquisition ℓ, the scatterers, indexed by r, are located at

$$\boldsymbol{y}_\epsilon^{\ell,r} = 100 e^{i\theta_y^{\ell,r}}, \quad 1 \le \ell \le L, \quad 1 \le r \le R, \tag{4.4}$$

where the $\theta_y^{\ell,r}$'s are independent and identically distributed with the uniform distribution over $(0, 2\pi)$. Let $\boldsymbol{Y}_\epsilon^\ell = \{\boldsymbol{y}_\epsilon^{\ell,r}\}_{r=1}^R$ denote the positions of all small scatterers at a given acquisition ℓ and define

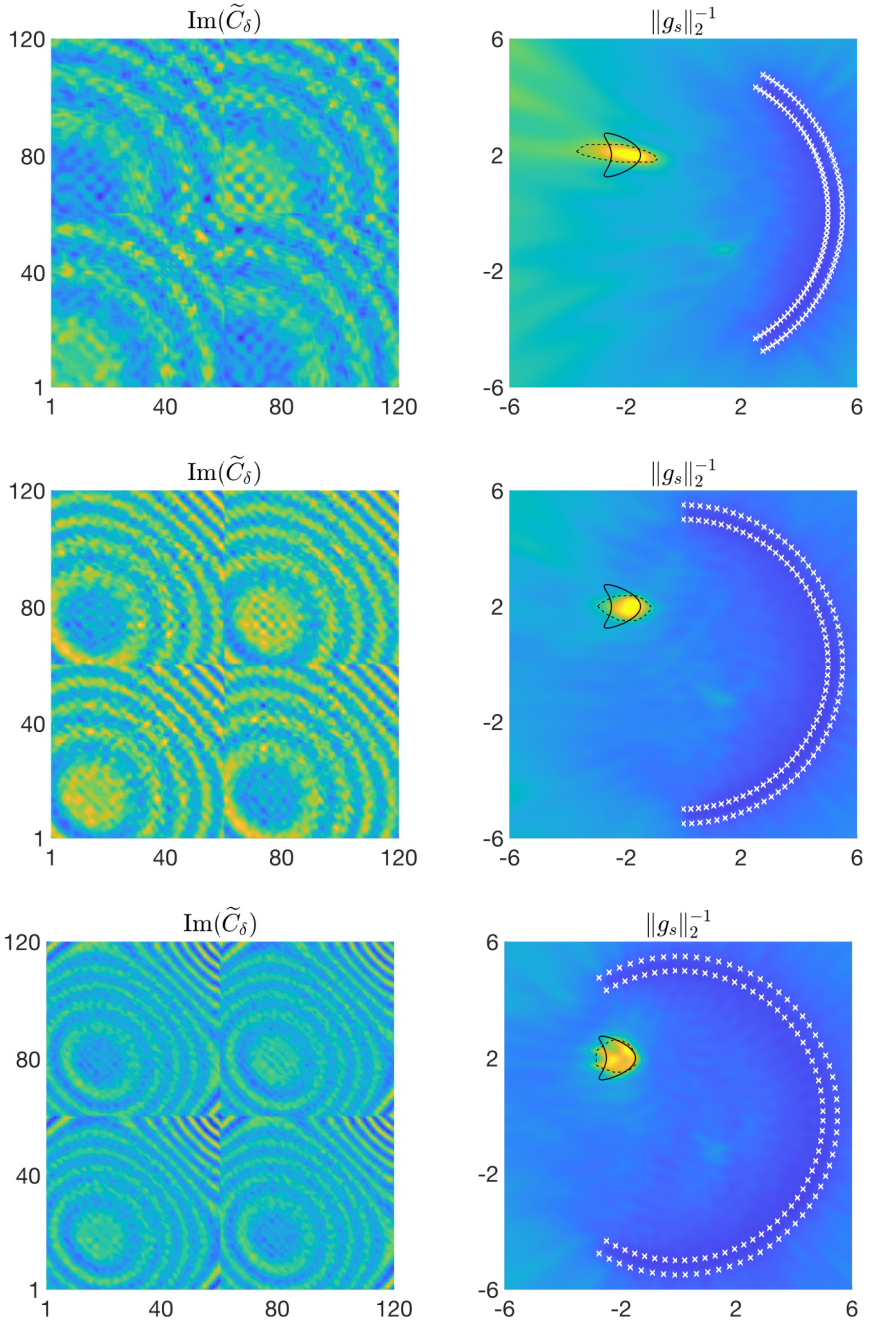

Figure 9. *In the case of limited-aperture measurements, achieving a perfect reconstruction of the shape is not anticipated. Here, the aperture is* $2\pi/3$ *in the top row,* π *in the middle row, and* $4\pi/3$ *in the bottom row. The dotted line corresponds to the convex hull of the level set of the indicator function that minimizes the area error. The error is minimized at* 0.54 *(top),* 0.45 *(middle), and* 0.62 *(bottom) times the maximum of the indicator function, with corresponding errors of* 3.51×10^{-2}, 2.10×10^{-2}, *and* 3.94×10^{-3}, *respectively.*

$$\tilde{v}_\epsilon(\boldsymbol{x}, \boldsymbol{Y}_\epsilon^\ell, \boldsymbol{z}_\epsilon) = \sum_{r=1}^{R} \tilde{v}_\epsilon(\boldsymbol{x}, \boldsymbol{y}_\epsilon^{\ell,r}, \boldsymbol{z}_\epsilon). \tag{4.5}$$

In this scenario, the scattered field w_ϵ^s reads

$$w_\epsilon^s(\boldsymbol{x}, \boldsymbol{Y}_\epsilon^\ell, \boldsymbol{z}_\epsilon) \approx u^s(\boldsymbol{x}, \boldsymbol{z}_\epsilon) + \tilde{v}_\epsilon(\boldsymbol{x}, \boldsymbol{Y}_\epsilon^\ell, \boldsymbol{z}_\epsilon). \tag{4.6}$$

We use the same technique to remove u^s and assemble the matrix

$$\widetilde{C}_{jm}^R = \frac{2ik|\Sigma_\epsilon|\sigma_\epsilon}{LR} \sum_{\ell=1}^{L} \overline{\tilde{v}_\epsilon(\boldsymbol{x}_j, \boldsymbol{Y}_\epsilon^\ell, \boldsymbol{z}_\epsilon)} \tilde{v}_\epsilon(\boldsymbol{x}_m, \boldsymbol{Y}_\epsilon^\ell, \boldsymbol{z}_\epsilon) - \left[\phi(\boldsymbol{x}_j, \boldsymbol{x}_m) - \overline{\phi(\boldsymbol{x}_j, \boldsymbol{x}_m)}\right]. \tag{4.7}$$

The results are shown in Figure 10 for $R = 5$ (top row) and $R = 30$ (bottom row), with $J = 120$ sensors described in (4.1), $L = 400$ realizations, and noise levels of 10^{-2} (top row) and 5×10^{-2}

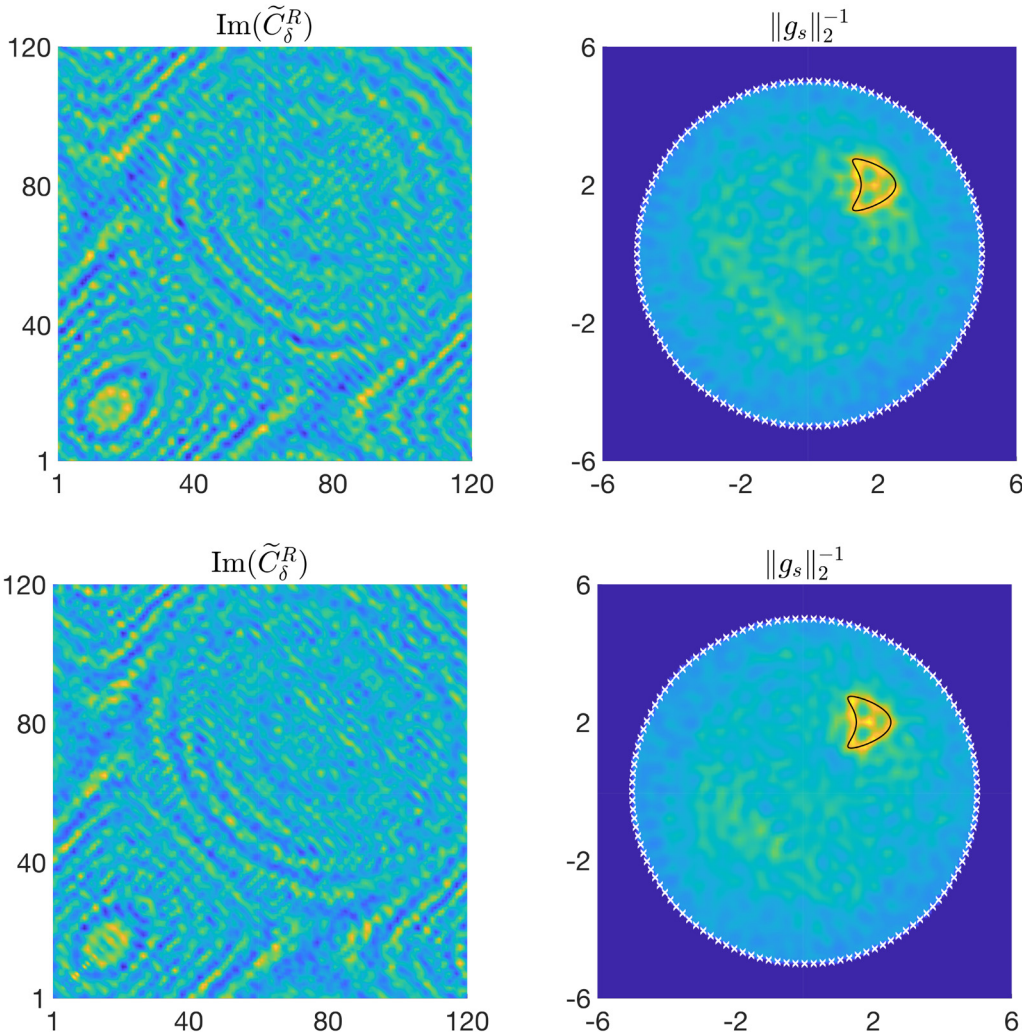

Figure 10. *When using several small scatterers, the signal is amplified by the number R of scatterers. With $R = 5$ random scatterers, we were able to increase the noise level from 5×10^{-3} to 10^{-2} (top row). With $R = 30$, we managed to raise the noise level to 5×10^{-2} (bottom row).*

(bottom row). This increased noise level is manageable because the signal magnitude within (4.5) is boosted by a factor of R compared to previous scenarios. This indicates a significant improvement and opens avenues for future endeavors.

5. Conclusions. We have introduced a novel version of the LSM as a powerful tool for addressing the sound-soft inverse scattering problem in two dimensions featuring randomly distributed small scatterers. Our approach is underpinned by a robust theoretical foundation, leveraging a rigorous asymptotic model and a modified Helmholtz–Kirchhoff identity, building upon our prior work on the LSM for random sources [18]. The implementation is comprehensive, incorporating essential components such as boundary elements, SVD, Tikhonov regularization, and Morozov's discrepancy principle. Finally, the numerical experiments presented in this paper demonstrate the effectiveness, accuracy, and robustness of our algorithms across various scenarios. The code used for generating the figures in the numerical experiments is available on GitHub at github.com/Hadrien-Montanelli/lsmlab.

This study has laid the groundwork for potential extensions and broader applications. The first avenue involves extending the developed framework to three dimensions and exploring its adaptability to different boundary conditions, enhancing the model's versatility. Additionally, expanding the model to encompass a continuous distribution of random scatterers on a surface would move us toward a more realistic configuration. This adjustment might also address the noise issues raised in the numerical experiments, although a detailed analysis of this aspect is beyond the paper's scope. The subsequent progression toward a heightened level of realism involves contemplating random scatterers distributed within a volume. Finally, we would like to extend our sampling method to elastic waves, enabling its application to subsurface imaging.

Appendix A. Auxiliary interior problem. Let $D_\epsilon = D_\epsilon(\boldsymbol{y}_\epsilon)$ denote the disk of radius $\lambda\epsilon$ centered at $\boldsymbol{y}_\epsilon$, as in section 2. Let $u_\epsilon \in H^1(D_\epsilon)$ be the solution to

$$\begin{cases} \Delta u_\epsilon + k^2 u_\epsilon = 0 & \text{in } D_\epsilon, \\ u_\epsilon = f & \text{on } \partial D_\epsilon, \end{cases} \tag{A.1}$$

for some $f \in H^{1/2}(\partial D_\epsilon)$. The corresponding single layer potential reads

$$\begin{aligned} &S_\epsilon : H^{-1/2}(\partial D_\epsilon) \to H^{1/2}(\partial D_\epsilon), \\ &S_\epsilon g(\boldsymbol{x}) = \int_{\partial D_\epsilon} \phi(\boldsymbol{x}, \boldsymbol{y}) g(\boldsymbol{y}) ds(\boldsymbol{y}), \quad \boldsymbol{x} \in \partial D_\epsilon, \end{aligned} \tag{A.2}$$

with $\phi(\boldsymbol{x}, \boldsymbol{y})$ as in (1.1). We now write $D_\epsilon = \boldsymbol{y}_\epsilon + \lambda\epsilon\widehat{D}$, where $\widehat{D}$ is the unit disk centered at the origin, and define the following change of variables:

$$\widehat{\boldsymbol{x}} = \frac{\boldsymbol{x} - \boldsymbol{y}_\epsilon}{\lambda\epsilon}, \quad \widehat{\boldsymbol{y}} = \frac{\boldsymbol{y} - \boldsymbol{y}_\epsilon}{\lambda\epsilon}, \quad \widehat{u}_\epsilon(\widehat{\boldsymbol{x}}) = u_\epsilon(\boldsymbol{y}_\epsilon + \lambda\epsilon\widehat{\boldsymbol{x}}). \tag{A.3}$$

Then, $\widehat{u}_\epsilon \in H^1(\widehat{D})$ satisfies

$$\begin{cases} \Delta \widehat{u}_\epsilon + 4\pi^2\epsilon^2 \widehat{u}_\epsilon = 0 & \text{in } \widehat{D}, \\ \widehat{u}_\epsilon = \widehat{f}_\epsilon & \text{on } \partial\widehat{D}, \end{cases} \tag{A.4}$$

with $\widehat{f}_\epsilon(\widehat{\boldsymbol{x}}) = f(\boldsymbol{y}_\epsilon + \lambda\epsilon\widehat{\boldsymbol{x}}) \in H^{1/2}(\partial\widehat{D})$. The associated single layer potential reads

$$\widehat{S}_\epsilon : H^{-1/2}(\partial\widehat{D}) \to H^{1/2}(\partial\widehat{D}),$$
$$\widehat{S}_\epsilon\widehat{g}(\widehat{\boldsymbol{x}}) = \int_{\partial\widehat{D}} \widehat{\phi}_\epsilon(\widehat{\boldsymbol{x}},\widehat{\boldsymbol{y}})\widehat{g}(\widehat{\boldsymbol{y}})ds(\widehat{\boldsymbol{y}}), \quad \widehat{\boldsymbol{x}} \in \partial\widehat{D}, \tag{A.5}$$

with

$$\widehat{\phi}_\epsilon(\widehat{\boldsymbol{x}},\widehat{\boldsymbol{y}}) = \phi(\boldsymbol{y}_\epsilon + \lambda\epsilon\widehat{\boldsymbol{x}}, \boldsymbol{y}_\epsilon + \lambda\epsilon\widehat{\boldsymbol{y}}) = \frac{i}{4}H_0^{(1)}(2\pi\epsilon|\widehat{\boldsymbol{x}} - \widehat{\boldsymbol{y}}|). \tag{A.6}$$

On $\partial\widehat{D}$, we can expand any $\widehat{f} \in H^{1/2}(\partial\widehat{D})$ as a Fourier series

$$\widehat{f}(\theta) = \frac{1}{\sqrt{2\pi}} \sum_{n=-\infty}^{+\infty} c_n e^{in\theta}, \quad \theta \in [0, 2\pi], \tag{A.7}$$

with Fourier coefficients

$$c_n = \frac{1}{2\pi}\int_0^{2\pi} \widehat{f}(\theta)e^{-in\theta}d\theta, \tag{A.8}$$

and define the $1/2$-norm as

$$\|\widehat{f}\|^2_{H^{1/2}(\partial\widehat{D})} = \sum_{n=-\infty}^{+\infty} |c_n|^2(1+n^2)^{1/2}. \tag{A.9}$$

Similarly, we can expand any $\widehat{g} \in H^{-1/2}(\partial\widehat{D})$ as a Fourier series

$$\widehat{g}(\theta) = \frac{1}{\sqrt{2\pi}} \sum_{n=-\infty}^{+\infty} d_n e^{in\theta}, \quad \theta \in [0, 2\pi], \tag{A.10}$$

and define the negative $1/2$-norm as

$$\|\widehat{g}\|^2_{H^{-1/2}(\partial\widehat{D})} = \sum_{n=-\infty}^{+\infty} |d_n|^2(1+n^2)^{-1/2}. \tag{A.11}$$

Finally, we define the duality pairing between $H^{1/2}(\partial\widehat{D})$ and $H^{-1/2}(\partial\widehat{D})$ via

$$\langle\widehat{f},\widehat{g}\rangle = \int_{\partial\widehat{D}} \widehat{f}(\widehat{\boldsymbol{y}})\overline{\widehat{g}(\widehat{\boldsymbol{y}})}ds(\widehat{\boldsymbol{y}}) = \sum_{n=-\infty}^{\infty} c_n d_n \tag{A.12}$$

for any $\widehat{f} \in H^{1/2}(\partial\widehat{D})$ and $\widehat{g} \in L^2(\partial\widehat{D})$. We extend it to $\widehat{g} \in H^{-1/2}(\partial\widehat{D})$ by density.

On ∂D_ϵ, we define the $1/2$-norm of any $f \in H^{1/2}(\partial D_\epsilon)$ via

$$\|f\|_{H^{1/2}(\partial D_\epsilon)} = \|\widehat{f}_\epsilon\|_{H^{1/2}(\partial\widehat{D})}, \tag{A.13}$$

where $\widehat{f}_\epsilon(\widehat{\boldsymbol{x}}) = f(\boldsymbol{y}_\epsilon + \lambda\epsilon\widehat{\boldsymbol{x}}) \in H^{1/2}(\partial\widehat{D})$. The duality pairing between the spaces $H^{1/2}(\partial D_\epsilon)$ and $H^{-1/2}(\partial D_\epsilon)$ is then defined via

$$\langle f, g\rangle = \int_{\partial D_\epsilon} f(\boldsymbol{y})\overline{g(\boldsymbol{y})}ds(\boldsymbol{y}) \tag{A.14}$$

for $f \in H^{1/2}(\partial D_\epsilon)$ and $g \in L^2(\partial D_\epsilon)$. We extend it to $g \in H^{-1/2}(\partial D_\epsilon)$ by density. This allows us to finally define

$$\|g\|_{H^{-1/2}(\partial D_\epsilon)} = \sup_{f\in H^{1/2}(\partial D_\epsilon)\neq 0} \frac{\langle f, g\rangle}{\|f\|_{H^{1/2}(\partial D_\epsilon)}}. \tag{A.15}$$

From the definitions above, we note that

$$\langle f, g\rangle = \int_{\partial D_\epsilon} f(\boldsymbol{y})\overline{g(\boldsymbol{y})}ds(\boldsymbol{y}) = \lambda\epsilon \int_{\partial\widehat{D}} \widehat{f}_\epsilon(\widehat{\boldsymbol{y}})\overline{\widehat{g}_\epsilon(\widehat{\boldsymbol{y}})}ds(\widehat{\boldsymbol{y}}) = \lambda\epsilon\langle\widehat{f}_\epsilon, \widehat{g}_\epsilon\rangle, \tag{A.16}$$

where $\widehat{f}_\epsilon(\widehat{\boldsymbol{x}}) = f(\boldsymbol{y}_\epsilon + \lambda\epsilon\widehat{\boldsymbol{x}})$ and $\widehat{g}_\epsilon(\widehat{\boldsymbol{x}}) = g(\boldsymbol{y}_\epsilon + \lambda\epsilon\widehat{\boldsymbol{x}})$, and hence

$$\|g\|_{H^{-1/2}(\partial D_\epsilon)} = \lambda\epsilon\|\widehat{g}_\epsilon\|_{H^{-1/2}(\partial\widehat{D})}. \tag{A.17}$$

Going back to the potentials, a direct calculation yields, for $g \in H^{-1/2}(\partial D_\epsilon)$,

$$\begin{aligned}\widehat{S_\epsilon g}(\widehat{\boldsymbol{x}}) = S_\epsilon g(\boldsymbol{y}_\epsilon + \lambda\epsilon\widehat{\boldsymbol{x}}) &= \int_{\partial D_\epsilon} \phi(\boldsymbol{y}_\epsilon + \lambda\epsilon\widehat{\boldsymbol{x}}, \boldsymbol{y})g(\boldsymbol{y})ds(\boldsymbol{y}),\\ &= \lambda\epsilon \int_{\partial\widehat{D}} \phi(\boldsymbol{y}_\epsilon + \lambda\epsilon\widehat{\boldsymbol{x}}, \boldsymbol{y}_\epsilon + \lambda\epsilon\widehat{\boldsymbol{y}})\widehat{g}_\epsilon(\widehat{\boldsymbol{y}})ds(\widehat{\boldsymbol{y}}),\\ &= \lambda\epsilon\widehat{S}_\epsilon\widehat{g}_\epsilon(\widehat{\boldsymbol{x}}).\end{aligned} \tag{A.18}$$

Finally, suppose that $g_\epsilon = S_\epsilon^{-1} f \in H^{-1/2}(\partial D_\epsilon)$ for some $f \in H^{1/2}(\partial D_\epsilon)$, then

$$S_\epsilon g_\epsilon = f \Rightarrow \widehat{S_\epsilon g_\epsilon} = \widehat{f}_\epsilon \Rightarrow \lambda\epsilon\widehat{S}_\epsilon\widehat{g}_\epsilon = \widehat{f}_\epsilon \Rightarrow \lambda\epsilon\widehat{g}_\epsilon = \widehat{S}_\epsilon^{-1}\widehat{f}_\epsilon \Rightarrow \lambda\epsilon\widehat{S_\epsilon^{-1} f} = \widehat{S}_\epsilon^{-1}\widehat{f}_\epsilon. \tag{A.19}$$

We summarize all the previous definitions and observations in the following lemma.

Lemma A.1. *For any function $f \in H^{1/2}(\partial D_\epsilon)$ and $g \in H^{-1/2}(\partial D_\epsilon)$, define*

$$\widehat{f}_\epsilon(\widehat{\boldsymbol{x}}) = f(\boldsymbol{y}_\epsilon + \lambda\epsilon\widehat{\boldsymbol{x}}) \in H^{1/2}(\partial\widehat{D}) \quad \textit{and} \quad \widehat{g}_\epsilon(\widehat{\boldsymbol{x}}) = g(\boldsymbol{y}_\epsilon + \lambda\epsilon\widehat{\boldsymbol{x}}) \in H^{-1/2}(\partial\widehat{D}). \tag{A.20}$$

Then

$$\|f\|_{H^{1/2}(\partial D_\epsilon)} = \|\widehat{f}_\epsilon\|_{H^{1/2}(\partial\widehat{D})} \quad \textit{and} \quad \|g\|_{H^{-1/2}(\partial D_\epsilon)} = \lambda\epsilon\|\widehat{g}_\epsilon\|_{H^{-1/2}(\partial\widehat{D})}, \tag{A.21}$$

as well as

$$\langle f, g\rangle = \lambda\epsilon\langle\widehat{f}_\epsilon, \widehat{g}_\epsilon\rangle, \quad \widehat{S_\epsilon g} = \lambda\epsilon\widehat{S}_\epsilon\widehat{g}_\epsilon, \quad \textit{and} \quad \lambda\epsilon\widehat{S_\epsilon^{-1} f} = \widehat{S}_\epsilon^{-1}\widehat{f}_\epsilon. \tag{A.22}$$

We now prove a result on the Fourier coefficients of functions defined on ∂D_ϵ.

Lemma A.2. *Let $f \in H^{1/2}(\partial D_\epsilon)$. Suppose that f can be smoothly extended to a twice continuously differentiable function in a neighborhood U_ϵ of D_ϵ and that there exists $r \geq 0$ and a constant $C > 0$, independent of ϵ, such that for small enough ϵ,*

$$\sup_{\boldsymbol{x} \in U_\epsilon} \left| \frac{\partial^{i+j} f}{\partial x^i \partial y^j}(\boldsymbol{x}) \right| \leq C\epsilon^r \tag{A.23}$$

for all integers $i, j \geq 0$ such that $i + j \leq 2$. Then, the Fourier coefficients of $\widehat{f}_\epsilon$ verify, for small enough ϵ,

$$c_0(\epsilon) = f(\boldsymbol{y}_\epsilon) + \mathcal{O}(\epsilon^{r+2}) \quad \text{and} \quad |c_n(\epsilon)| \leq C\frac{\epsilon^{r+1}}{|n|^2} \quad \forall n \neq 0, \tag{A.24}$$

where $C > 0$ is a constant independent of n and ϵ.

Proof. Since f is twice continuously differentiable in U_ϵ and its second derivatives are uniformly bounded by a quantity $\mathcal{O}(\epsilon^r)$, we have that

$$f(\boldsymbol{y}_\epsilon + \lambda\epsilon e^{i\theta}) = f(\boldsymbol{y}_\epsilon) + \lambda\epsilon\cos\theta\frac{\partial f}{\partial x}(\boldsymbol{y}_\epsilon) + \lambda\epsilon\sin\theta\frac{\partial f}{\partial x}(\boldsymbol{y}_\epsilon) + \mathcal{O}(\epsilon^{r+2}), \tag{A.25}$$

and hence

$$c_0(\epsilon) = \frac{1}{2\pi}\int_0^{2\pi} f(\boldsymbol{y}_\epsilon + \lambda\epsilon e^{i\theta})d\theta = f(\boldsymbol{y}_\epsilon) + \mathcal{O}(\epsilon^{r+2}). \tag{A.26}$$

Moreover, because $\theta \mapsto \widehat{f}_\epsilon(\theta) = f(\boldsymbol{y}_\epsilon + \lambda\epsilon e^{i\theta})$ is twice continuously differentiable, its first derivative has bounded variation

$$V_\epsilon = \int_0^{2\pi} \left| \frac{d^2}{d\theta^2}\widehat{f}_\epsilon(\theta) \right| d\theta, \tag{A.27}$$

and its Fourier coefficients satisfy [33, Thm. 4.1]

$$|c_n(\epsilon)| \leq \frac{V_\epsilon}{2\pi|n|^2} \quad \forall n \neq 0. \tag{A.28}$$

It suffices to estimate V_ϵ to conclude. Let

$$x_\epsilon(\theta) = \lambda\epsilon^{-p}\cos\theta_y + \lambda\epsilon\cos\theta, \quad y_\epsilon(\theta) = \lambda\epsilon^{-p}\sin\theta_y + \lambda\epsilon\sin\theta, \quad \theta \in [0, 2\pi]. \tag{A.29}$$

Since $\widehat{f}_\epsilon(\theta) = f(x_\epsilon(\theta), y_\epsilon(\theta))$, we have that

$$\frac{d}{d\theta}\widehat{f}_\epsilon(\theta) = \lambda\epsilon\left[-\sin\theta\frac{\partial f}{\partial x}(x_\epsilon(\theta), y_\epsilon(\theta)) + \cos\theta\frac{\partial f}{\partial y}(x_\epsilon(\theta), y_\epsilon(\theta))\right] \tag{A.30}$$

and

$$\frac{d^2}{d\theta^2}\widehat{f}_\epsilon(\theta) = \lambda\epsilon\left[-\cos\theta\frac{\partial f}{\partial x}(x_\epsilon(\theta), y_\epsilon(\theta)) - \sin\theta\frac{\partial f}{\partial y}(x_\epsilon(\theta), y_\epsilon(\theta))\right] + \mathcal{O}(\epsilon^{r+2}), \tag{A.31}$$

since the second derivatives are uniformly bounded by a quantity $\mathcal{O}(\epsilon^r)$. Therefore, there exists a constant $C>0$, independent of ϵ, such that for small enough ϵ, $V_\epsilon \le C\epsilon^{r+1}$. ∎

We note that if we assume that f can be smoothly extended to an infinitely differentiable function and that all of its derivatives are uniformly bounded by a quantity $\mathcal{O}(\epsilon^r)$, then we can show that $|c_n(\epsilon)| \le C\epsilon^{r+1}/|n|^{1+\nu}$ for all $n \neq 0$ and any integer $\nu > 0$.

Let $S_\epsilon^{-1} : H^{1/2}(\partial D_\epsilon) \to H^{-1/2}(\partial D_\epsilon)$ and $\widehat{S}_\epsilon^{-1} : H^{1/2}(\partial \widehat{D}) \to H^{-1/2}(\partial \widehat{D})$ be the inverse operators of (A.2) and (A.5).

Theorem A.3. *If $\widehat{f}$ has Fourier coefficients c_n, then $\widehat{S}_\epsilon^{-1}\widehat{f}$ has Fourier coefficients*

$$d_n = -\frac{2i}{\pi}\frac{c_n}{J_n(2\pi\epsilon)H_n^{(1)}(2\pi\epsilon)}, \quad n \in \mathbb{Z}. \tag{A.32}$$

Moreover, there exists a constant $C>0$, independent of ϵ, such that for small enough ϵ,

$$\|\widehat{S}_\epsilon^{-1}\| \le C \quad \text{and} \quad \|S_\epsilon^{-1}\| \le C. \tag{A.33}$$

If $\widehat{f}_\epsilon(\widehat{\boldsymbol{x}}) = f(\boldsymbol{y}_\epsilon + \lambda\epsilon\widehat{\boldsymbol{x}})$ for some function f that verifies the assumptions of Lemma A.2, then there exists a constant $C>0$, independent of n and ϵ, such that for small enough ϵ,

$$|d_0(\epsilon)| \le C|\log\epsilon|^{-1}|f(\boldsymbol{y}_\epsilon)| + \mathcal{O}(|\log\epsilon|^{-1}\epsilon^{r+2}) \quad \text{and} \quad |d_n(\epsilon)| \le C\frac{\epsilon^{r+1}}{|n|} \quad \forall n \neq 0. \tag{A.34}$$

Moreover, there exists a constant $C>0$, independent of ϵ, such that for small enough ϵ,

$$\|S_\epsilon^{-1}f\|_{H^{-1/2}(\partial D_\epsilon)} \le C|\log(\epsilon)|^{-1}|f(\boldsymbol{y}_\epsilon)| + \mathcal{O}(\epsilon^{r+1}). \tag{A.35}$$

Proof. Let $\widehat{u}_\epsilon \in H^1(\widehat{D}) \cup H^1_{\mathrm{loc}}(\mathbb{R}^2 \setminus \overline{\widehat{D}})$ be the solution to

$$\begin{cases} \Delta\widehat{u}_\epsilon + 4\pi^2\epsilon^2\widehat{u}_\epsilon = 0 & \text{in } \mathbb{R}^2 \setminus \partial\widehat{D}, \\ \widehat{u}_\epsilon = \widehat{f} & \text{on } \partial\widehat{D}, \\ \widehat{u}_\epsilon \text{ is radiating}, \end{cases} \tag{A.36}$$

for some $\widehat{f} \in H^{1/2}(\partial\widehat{D})$ with

$$\widehat{f}(\theta) = \frac{1}{\sqrt{2\pi}}\sum_{n=-\infty}^{+\infty} c_n e^{in\theta}, \quad \theta \in [0, 2\pi]. \tag{A.37}$$

We look for a solution of the form

$$\widehat{u}_\epsilon(r,\theta) = \sum_{n=-\infty}^{+\infty} \alpha_n(\epsilon)J_n(2\pi\epsilon r)e^{in\theta} \quad \text{in } \widehat{D}, \tag{A.38}$$

and

$$\widehat{u}_\epsilon(r,\theta) = \sum_{n=-\infty}^{+\infty} \beta_n(\epsilon)H_n^{(1)}(2\pi\epsilon r)e^{in\theta} \quad \text{in } \mathbb{R}^2 \setminus \overline{\widehat{D}}, \tag{A.39}$$

with $\widehat{u}_\epsilon = \widehat{S}_\epsilon \widehat{g}_\epsilon$. The boundary condition $\widehat{u}_\epsilon = \widehat{S}_\epsilon \widehat{g}_\epsilon = \widehat{f}$ on $\partial\widehat{D}$ yields

$$\widehat{u}_\epsilon(r,\theta) = \frac{1}{\sqrt{2\pi}} \sum_{n=-\infty}^{+\infty} \frac{c_n}{J_n(2\pi\epsilon)} J_n(2\pi\epsilon r) e^{in\theta} \quad \text{in } \widehat{D}, \tag{A.40}$$

and

$$\widehat{u}_\epsilon(r,\theta) = \frac{1}{\sqrt{2\pi}} \sum_{n=-\infty}^{+\infty} \frac{c_n}{H_n^{(1)}(2\pi\epsilon)} H_n^{(1)}(2\pi\epsilon r) e^{in\theta} \quad \text{in } \mathbb{R}^2 \setminus \overline{\widehat{D}}. \tag{A.41}$$

Note that $\widehat{S}_\epsilon^{-1} : \widehat{f} \to \widehat{S}_\epsilon^{-1}\widehat{f}$ with

$$\widehat{S}_\epsilon^{-1}\widehat{f}(\theta) = \left[\frac{\partial \widehat{u}_\epsilon}{\partial n}\right](\theta) = \sum_{n=-\infty}^{+\infty} \sqrt{2\pi\epsilon} c_n \left(\frac{J_n'(2\pi\epsilon)}{J_n(2\pi\epsilon)} - \frac{H_n^{(1)'}(2\pi\epsilon)}{H_n^{(1)}(2\pi\epsilon)} \right) e^{in\theta}, \quad \theta \in [0, 2\pi], \tag{A.42}$$

where $[\partial\widehat{u}_\epsilon/\partial n]$ denotes the jump of the conormal derivative through $\partial\widehat{D}$. We note that

$$\frac{J_n'(2\pi\epsilon)}{J_n(2\pi\epsilon)} - \frac{H_n^{(1)'}(2\pi\epsilon)}{H_n^{(1)}(2\pi\epsilon)} = -\frac{i}{\pi^2\epsilon} \frac{1}{J_n(2\pi\epsilon) H_n^{(1)}(2\pi\epsilon)} \quad \forall n, \tag{A.43}$$

using the Wronskian (see, e.g., [1, eq. (9.1.16)]). This yields

$$\widehat{S}_\epsilon^{-1}\widehat{f}(\theta) = -\frac{1}{\sqrt{2\pi}} \frac{2i}{\pi} \sum_{n=-\infty}^{+\infty} \frac{c_n}{J_n(2\pi\epsilon) H_n^{(1)}(2\pi\epsilon)} e^{in\theta}, \quad \theta \in [0, 2\pi], \tag{A.44}$$

which shows that the Fourier coefficients of $\widehat{S}_\epsilon^{-1}\widehat{f}$ are given by

$$d_n = -\frac{2i}{\pi} \frac{c_n}{J_n(2\pi\epsilon) H_n^{(1)}(2\pi\epsilon)}, \quad n \in \mathbb{Z}. \tag{A.45}$$

From the coefficients d_n, it is clear that the squared negative 1/2-norm reads

$$\|\widehat{S}_\epsilon^{-1}\widehat{f}\|^2_{H^{-1/2}(\partial\widehat{D})} = \frac{4}{\pi^2} \sum_{n=-\infty}^{+\infty} \frac{|c_n|^2}{|J_n(2\pi\epsilon) H_n^{(1)}(2\pi\epsilon)|^2} (1+n^2)^{-1/2}. \tag{A.46}$$

We choose an integer N such that the uniform estimates of Lemma C.4 hold and split the norm as follows:

$$\begin{aligned} \|\widehat{S}_\epsilon^{-1}\widehat{f}\|^2_{H^{-1/2}(\partial\widehat{D})} = {} & \frac{4}{\pi^2} \sum_{|n|<N} \frac{|c_n|^2}{|J_n(2\pi\epsilon) H_n^{(1)}(2\pi\epsilon)|^2} (1+n^2)^{-1/2} \\ & + \frac{4}{\pi^2} \sum_{|n|\geq N} \frac{|c_n|^2}{|J_n(2\pi\epsilon) H_n^{(1)}(2\pi\epsilon)|^2} (1+n^2)^{-1/2}. \end{aligned} \tag{A.47}$$

We use the asymptotics for small arguments of Lemma C.2 for $n = 0$,

$$\frac{1}{|J_0(2\pi\epsilon) H_0^{(1)}(2\pi\epsilon)|} \leq C |\log\epsilon|^{-1} \leq 1, \tag{A.48}$$

with a constant $C>0$ independent of ϵ, as well as for $1\le|n|<N$,

$$\frac{1}{|J_n(2\pi\epsilon)H_n^{(1)}(2\pi\epsilon)|}\le Cn, \tag{A.49}$$

with a constant $C>0$ independent of n and ϵ (it is the maximum over $1\le|n|<N$ of the constants appearing for each n). For $|n|\ge N$, we use the uniform estimates of Lemma C.4,

$$\frac{1}{|J_n(2\pi\epsilon)H_n^{(1)}(2\pi\epsilon)|}\le Cn, \tag{A.50}$$

with a constant $C>0$ independent of n and ϵ. Putting the pieces together yields

$$\|\widehat{S}_\epsilon^{-1}\widehat{f}\|^2_{H^{-1/2}(\partial\widehat{D})}\le C\sum_{n=-\infty}^{+\infty}|c_n|^2(1+n^2)^{1/2}=C\|f\|^2_{H^{1/2}(\partial\widehat{D})}, \tag{A.51}$$

that is, $\|\widehat{S}_\epsilon^{-1}\|\le C$. For S_ϵ^{-1}, from Lemma A.1, we observe that, for any $f\in H^{1/2}(\partial D_\epsilon)$,

$$\|S_\epsilon^{-1}f\|_{H^{-1/2}(\partial D_\epsilon)}=\lambda\epsilon\|\widehat{S_\epsilon^{-1}f}\|_{H^{-1/2}(\partial\widehat{D})}=\|\widehat{S}_\epsilon^{-1}\widehat{f}_\epsilon\|_{H^{-1/2}(\partial\widehat{D})}, \tag{A.52}$$

with $\widehat{f}_\epsilon(\widehat{\boldsymbol{x}})=f(\boldsymbol{y}_\epsilon+\lambda\epsilon\widehat{\boldsymbol{x}})\in H^{1/2}(\partial\widehat{D})$. This yields

$$\|S_\epsilon^{-1}f\|_{H^{-1/2}(\partial D_\epsilon)}\le C\|\widehat{f}_\epsilon\|_{H^{1/2}(\partial\widehat{D})}=C\|f\|_{H^{1/2}(\partial D_\epsilon)}. \tag{A.53}$$

If $\widehat{f}_\epsilon(\widehat{\boldsymbol{x}})=f(\boldsymbol{y}_\epsilon+\lambda\epsilon\widehat{\boldsymbol{x}})$ for some function f that verifies the assumptions of Lemma A.2, then there exists a constant $C>0$, independent of n and ϵ, such that for small enough ϵ, the Fourier coefficients of $\widehat{f}_\epsilon$ satisfy

$$c_0(\epsilon)=f(\boldsymbol{y}_\epsilon)+\mathcal{O}(\epsilon^{r+2})\quad\text{and}\quad|c_n(\epsilon)|\le C\frac{\epsilon^{r+1}}{|n|^2}\quad\forall n\ne0. \tag{A.54}$$

We choose, again, an integer N such that the uniform estimates of Lemma C.4 hold, and then combine the asymptotics for small arguments of Lemma C.2 for $n=0$ and $0\ne|n|\le N$ with the uniform estimates for $|n|\ge N$. This yields, for small enough ϵ,

$$|d_0(\epsilon)|\le C|\log\epsilon|^{-1}|f(\boldsymbol{y}_\epsilon)|+\mathcal{O}(|\log\epsilon|^{-1}\epsilon^{r+2})\quad\text{and}\quad|d_n(\epsilon)|\le C\frac{\epsilon^{r+1}}{|n|}\quad\forall n\ne0, \tag{A.55}$$

with a constant $C>0$ independent of n and ϵ. This immediately implies that

$$\|S_\epsilon^{-1}f\|_{H^{-1/2}(\partial D_\epsilon)}=\|\widehat{S}_\epsilon^{-1}\widehat{f}_\epsilon\|_{H^{-1/2}(\partial\widehat{D})}\le C|\log(\epsilon)|^{-1}|f(\boldsymbol{y}_\epsilon)|+\mathcal{O}(\epsilon^{r+1}). \tag{A.56}$$

■

Appendix B. Auxiliary exterior problem.

Let $D_\epsilon=D_\epsilon(\boldsymbol{y}_\epsilon)$ and $D=D(\mathbf{0})$ satisfy the assumptions of section 2. Let $w_\epsilon\in H^1_{\rm loc}(\mathbb{R}^s\setminus\{D\cup D_\epsilon\})$ be the solution to

$$\text{(B.1)}\qquad \begin{cases} \Delta w_\epsilon + k^2 w_\epsilon = 0 \quad \text{in } \mathbb{R}^2 \setminus \{\overline{D \cup D_\epsilon}\}, \\ w_\epsilon = f \quad \text{on } \partial D, \\ w_\epsilon = 0 \quad \text{on } \partial D_\epsilon, \\ w_\epsilon \text{ is radiating}, \end{cases}$$

for some $f \in H^{1/2}(\partial D)$. We seek to evaluate the solution w_ϵ in the domain B, characterized in section 2, via $w_\epsilon = \mathscr{S} g_\epsilon + \mathscr{S}_\epsilon h_\epsilon$ with operators

$$\text{(B.2)}\qquad \mathscr{S} : H^{-1/2}(\partial D) \to H^1(B),$$
$$\mathscr{S} g(\boldsymbol{x}) = \int_{\partial D} \phi(\boldsymbol{x}, \boldsymbol{y}) g(\boldsymbol{y}) ds(\boldsymbol{y}), \quad \boldsymbol{x} \in B,$$

and

$$\text{(B.3)}\qquad \mathscr{S}_\epsilon : H^{-1/2}(\partial D_\epsilon) \to H^1(B),$$
$$\mathscr{S}_\epsilon g(\boldsymbol{x}) = \int_{\partial D_\epsilon} \phi(\boldsymbol{x}, \boldsymbol{y}) g(\boldsymbol{y}) ds(\boldsymbol{y}), \quad \boldsymbol{x} \in B.$$

To solve (B.1), we must have

$$\text{(B.4)}\qquad S g_\epsilon + T_\epsilon h_\epsilon = f \quad \text{on } \partial D \quad \text{and} \quad S_\epsilon h_\epsilon + T_\epsilon^T g_\epsilon = 0 \quad \text{on } \partial D_\epsilon$$

with operators

$$\text{(B.5)}\qquad S : H^{-1/2}(\partial D) \to H^{1/2}(\partial D),$$
$$S g(\boldsymbol{x}) = \int_{\partial D} \phi(\boldsymbol{x}, \boldsymbol{y}) g(\boldsymbol{y}) ds(\boldsymbol{y}), \quad \boldsymbol{x} \in \partial D,$$

$$\text{(B.6)}\qquad S_\epsilon : H^{-1/2}(\partial D_\epsilon) \to H^{1/2}(\partial D_\epsilon),$$
$$S_\epsilon g(\boldsymbol{x}) = \int_{\partial D_\epsilon} \phi(\boldsymbol{x}, \boldsymbol{y}) g(\boldsymbol{y}) ds(\boldsymbol{y}), \quad \boldsymbol{x} \in \partial D_\epsilon,$$

$$\text{(B.7)}\qquad T_\epsilon : H^{-1/2}(\partial D_\epsilon) \to H^{1/2}(\partial D),$$
$$T_\epsilon g(\boldsymbol{x}) = \int_{\partial D_\epsilon} g(\boldsymbol{x}, \boldsymbol{y}) g(\boldsymbol{y}) ds(\boldsymbol{y}), \quad \boldsymbol{x} \in \partial D,$$

and

$$\text{(B.8)}\qquad T_\epsilon^T : H^{-1/2}(\partial D) \to H^{1/2}(\partial D_\epsilon),$$
$$T_\epsilon^T g(\boldsymbol{x}) = \int_{\partial D} \phi(\boldsymbol{x}, \boldsymbol{y}) g(\boldsymbol{y}) ds(\boldsymbol{y}), \quad \boldsymbol{x} \in \partial D_\epsilon.$$

This yields

$$\text{(B.9)}\qquad g_\epsilon = (I - S^{-1} T_\epsilon S_\epsilon^{-1} T_\epsilon^T)^{-1} S^{-1} f \quad \text{on } \partial D \quad \text{and} \quad h_\epsilon = -S_\epsilon^{-1} T_\epsilon^T g_\epsilon \quad \text{on } \partial D_\epsilon.$$

Both S^{-1} and S_ϵ^{-1} are continuous operators (see Theorem A.3 for the latter). Let

$$\text{(B.10)}\qquad A_\epsilon = S^{-1} T_\epsilon S_\epsilon^{-1} T_\epsilon^T : H^{-1/2}(\partial D) \to H^{-1/2}(\partial D).$$

We characterize, below, the norms of T_ϵ, T_ϵ^T, A_ϵ, $\mathscr{S}$, and $\mathscr{S}_\epsilon$.

Lemma B.1. *There exists a constant $C>0$, independent of ϵ, such that for small enough ϵ,*

$$\|T_\epsilon\| \le C\epsilon^{p/2},\ \|T_\epsilon^T\| \le C\epsilon^{p/2},\ \|A_\epsilon\| \le C\epsilon^{p},\ \|\mathscr{S}\| \le C,\ \text{and } \|\mathscr{S}_\epsilon\| \le C\epsilon^{p/2}. \tag{B.11}$$

If $g_\epsilon = S_\epsilon^{-1} f$ for some function f that verifies the assumptions of Lemma A.2, then there exists a constant $C>0$, independent of ϵ, such that for small enough ϵ,

$$\|T_\epsilon g_\epsilon\|_{H^{1/2}(\partial D)} \le C|\log\epsilon|^{-1}\epsilon^{p/2}|f(\boldsymbol{y}_\epsilon)| + \mathcal{O}(\epsilon^{p/2}\epsilon^r\epsilon^2) \tag{B.12}$$

and

$$\|\mathscr{S}_\epsilon g_\epsilon\|_{H^1(B)} \le C|\log\epsilon|^{-1}\epsilon^{p/2}|f(\boldsymbol{y}_\epsilon)| + \mathcal{O}(\epsilon^{p/2}\epsilon^r\epsilon^2). \tag{B.13}$$

Proof. To show that $\|T_\epsilon\|$ is small, we observe that, via Lemma C.3, for $\boldsymbol{x}\in\partial D$,

$$|T_\epsilon g(\boldsymbol{x})| \le \sup_{\boldsymbol{y}\in\partial D_\epsilon} |\phi(\boldsymbol{x},\boldsymbol{y})| \int_{\partial D_\epsilon} |g(\boldsymbol{y})| ds(\boldsymbol{y}) \le C\epsilon^{p/2}\|g\|_{H^{-1/2}(\partial D_\epsilon)}, \tag{B.14}$$

which leads to $\|T_\epsilon g\|_{L^2(\partial D)} \le C\epsilon^{p/2}$. Similarly, we can write, for $\boldsymbol{x}\in\partial D$,

$$|\nabla(T_\epsilon g)(\boldsymbol{x})| \le \sup_{\boldsymbol{y}\in\partial D_\epsilon} |\nabla_{\boldsymbol{x}}\phi(\boldsymbol{x},\boldsymbol{y})| \int_{\partial D_\epsilon} |g(\boldsymbol{y})| ds(\boldsymbol{y}) \le C\epsilon^{p/2}\|g\|_{H^{-1/2}(\partial D_\epsilon)}, \tag{B.15}$$

which leads to $\|\nabla(T_\epsilon g)\|_{L^2(\partial D)} \le C\epsilon^{p/2}$. This yields, since $T_\epsilon g \in H^s(\partial D)$ for any $s\ge 0$,

$$\|T_\epsilon g\|^2_{H^{1/2}(\partial D)} \le C\|T_\epsilon g\|^2_{H^1(\partial D)} = C\{\|T_\epsilon g\|^2_{L^2(\partial D)} + \|\nabla(T_\epsilon g)\|^2_{L^2(\partial D)}\} \le C\epsilon^p. \tag{B.16}$$

The same reasoning can be applied to T_ϵ^T. This immediately gives a bound on $\|A_\epsilon\|$.

For $\mathscr{S}$ and $\mathscr{S}_\epsilon$, we obtain for $x\in B$ the estimates

$$|\mathscr{S} g(\boldsymbol{x})| \le \sup_{\boldsymbol{y}\in\partial D} |\phi(\boldsymbol{x},\boldsymbol{y})| \int_{\partial D} |g(\boldsymbol{y})| ds(\boldsymbol{y}) \le C\|g\|_{H^{-1/2}(\partial D)} \tag{B.17}$$

and

$$|\mathscr{S}_\epsilon g(\boldsymbol{x})| \le \sup_{\boldsymbol{y}\in\partial D_\epsilon} |\phi(\boldsymbol{x},\boldsymbol{y})| \int_{\partial D_\epsilon} |g(\boldsymbol{y})| ds(\boldsymbol{y}) \le C\epsilon^{p/2}\|g\|_{H^{-1/2}(\partial D_\epsilon)} \tag{B.18}$$

and similar ones for their gradients.

Let $g_\epsilon = S_\epsilon^{-1} f$ for some function f that verifies the assumptions of Lemma A.2 and, for $\boldsymbol{x}\in\partial D$, let us write $T_\epsilon g_\epsilon(\boldsymbol{x})$ as a duality pairing

$$T_\epsilon g_\epsilon(\boldsymbol{x}) = \langle \phi(\boldsymbol{x},\cdot), S_\epsilon^{-1} f\rangle \tag{B.19}$$

between $\phi(\boldsymbol{x},\cdot)\in H^{1/2}(\partial D_\epsilon)$ and $S_\epsilon^{-1} f \in H^{-1/2}(\partial D_\epsilon)$. Then, via Lemma A.1,

$$T_\epsilon g_\epsilon(\boldsymbol{x}) = \lambda\epsilon\langle \widehat{\phi}_\epsilon(\boldsymbol{x},\cdot), \widehat{S_\epsilon^{-1} f}\rangle = \langle \widehat{\phi}_\epsilon(\boldsymbol{x},\cdot), \widehat{S}_\epsilon^{-1}\widehat{f}_\epsilon\rangle = \sum_{n=-\infty}^{\infty} c_n\overline{d_n}, \tag{B.20}$$

where c_n and d_n are the Fourier coefficients of $\widehat{\phi}_\epsilon(\boldsymbol{x},\widehat{\boldsymbol{y}}) = \phi(\boldsymbol{x},\boldsymbol{y}_\epsilon + \lambda\epsilon\widehat{\boldsymbol{y}})$ and $\widehat{S}_\epsilon^{-1}\widehat{f}_\epsilon$. Using Lemma A.2 for c_n and Theorem A.3 and d_n, there exists a constant $C>0$, independent of n and ϵ, such that for small enough ϵ,

$$c_0(\epsilon) = \phi(\boldsymbol{x},\boldsymbol{y}_\epsilon) + \mathcal{O}(\epsilon^{p/2+2}) = \mathcal{O}(\epsilon^{p/2}) \quad \text{and} \quad |c_n(\epsilon)| \le C\frac{\epsilon^{p/2+1}}{|n|^2} \quad \forall n \neq 0, \tag{B.21}$$

$$|d_0(\epsilon)| \le C|\log\epsilon|^{-1}|f(\boldsymbol{y}_\epsilon)| + \mathcal{O}(|\log\epsilon|^{-1}\epsilon^{r+2}) \quad \text{and} \quad |d_n(\epsilon)| \le C\frac{\epsilon^{r+1}}{|n|} \quad \forall n \neq 0.$$

Therefore, we have

$$|T_\epsilon g_\epsilon(\boldsymbol{x})| \le C|\log\epsilon|^{-1}\epsilon^{p/2}|f(\boldsymbol{y}_\epsilon)| + \mathcal{O}(\epsilon^{p/2}\epsilon^r\epsilon^2). \tag{B.22}$$

We have the same estimate for the gradient and hence

$$\|T_\epsilon g_\epsilon\|_{H^{1/2}(\partial D)} \le C|\log\epsilon|^{-1}\epsilon^{p/2}|f(\boldsymbol{y}_\epsilon)| + \mathcal{O}(\epsilon^{p/2}\epsilon^r\epsilon^2). \tag{B.23}$$

The proof for $\|\mathscr{S}_\epsilon g_\epsilon\|_{H^1(B)}$ is (almost) identical. ∎

Theorem B.2. *There exists a constant $C>0$, independent of ϵ, such that for small enough ϵ,*

$$\|w_\epsilon\|_{H^1(B)} \le C\|f\|_{H^{1/2}(\partial D)}. \tag{B.24}$$

Proof. We first write

$$\|w_\epsilon\|_{H^1(B)} \le \|\mathscr{S} g_\epsilon\|_{H^1(B)} + \|\mathscr{S}_\epsilon h_\epsilon\|_{H^1(B)} \tag{B.25}$$

and use Lemma B.1 to get

$$\|w_\epsilon\|_{H^1(B)} \le C\|g_\epsilon\|_{H^{-1/2}(\partial D)} + C\epsilon^{p/2}\|h_\epsilon\|_{H^{-1/2}(\partial D_\epsilon)} \tag{B.26}$$

with a constant $C>0$ independent of ϵ. From (B.9) and Lemma B.1, we observe that

$$\|g_\epsilon\|_{H^{-1/2}(\partial D)} \le C\|(I-A_\epsilon)^{-1}\|\,\|S^{-1}\|\,\|f\|_{H^{1/2}(\partial D)} \le C\|f\|_{H^{1/2}(\partial D)}, \tag{B.27}$$

since $\|A_\epsilon\| \le C\epsilon^{p/2} \le 1/2$ and $\|(I-A_\epsilon)^{-1}\| \le (1-\|A_\epsilon\|)^{-1} \le 2$ for small enough ϵ, and

$$\|h_\epsilon\|_{H^{-1/2}(\partial D_\epsilon)} \le C\|S_\epsilon^{-1}\|\,\|T_\epsilon^T\|\,\|g_\epsilon\|_{H^{-1/2}(\partial D)} \le C\epsilon^{p/2}\|f\|_{H^{1/2}(\partial D)}. \tag{B.28}$$

This yields

$$\|w_\epsilon\|_{H^1(B)} \le C\|f\|_{H^{1/2}(\partial D)} + C\epsilon^p\|f\|_{H^{1/2}(\partial D)} \le C\|f\|_{H^{1/2}(\partial D)}. \tag{B.29}$$

∎

Appendix C. Asymptotic formulas. Here, we revisit several helpful asymptotic formulas. Due to the symmetry relations that follow, our focus can be solely on positive integers $n \in \mathbb{N}$.

Lemma C.1 (symmetry relations). *For all $n \in \mathbb{N}$,*

$$J_{-n}(x) = (-1)^n J_n(x) \quad \forall x \in \mathbb{R} \quad \textit{and} \quad H_{-n}^{(1)}(x) = (-1)^n H_n^{(1)}(x) \quad \forall x \in (0,+\infty). \tag{C.1}$$

Lemma C.2 (asymptotics for small argument). *When $n \in \mathbb{N}$ is fixed and $x \to 0^+$,*

$$J_n(x) = \frac{1}{n!}\left(\frac{x}{2}\right)^n + \mathcal{O}(x^{n+1}) \quad \forall n \neq 0, \quad J_0(x) = 1 + \mathcal{O}(x^2), \tag{C.2}$$

$$H_n(x) = \frac{(n-1)!}{i\pi}\left(\frac{2}{x}\right)^n + \mathcal{O}\left(\frac{1}{x^{n-1}}\right) \quad \forall n \neq 0, \quad H_0(x) = \frac{2i}{\pi}\log\left(\frac{x}{2}\right) + \mathcal{O}(1). \tag{C.3}$$

Proof. See, e.g., [1, eqs. (9.1.7)–(9.1.9)]. ∎

Let us emphasize that the estimates in Lemma C.2 are not uniform in n, that is, the constants in the $\mathcal{O}$ are independent of $x \to 0^+$ but do depend on n.

Lemma C.3 (asymptotics for large argument). *When $n \in \mathbb{N}$ is fixed and $x \to +\infty$,*

$$J_n(x) = \sqrt{\frac{2}{\pi x}}\cos(x - n\pi/2 - \pi/4)\left(1 + \mathcal{O}\left(\frac{1}{x}\right)\right), \tag{C.4}$$

$$H_n^{(1)}(x) = \sqrt{\frac{2}{\pi x}}e^{i(x - n\pi/2 - \pi/4)}\left(1 + \mathcal{O}\left(\frac{1}{x}\right)\right). \tag{C.5}$$

Proof. See, e.g., [1, eqs. (9.2.1)–(9.2.3)]. ∎

The estimates in Lemma C.3 are not uniform in n either.

Lemma C.4 (asymptotics for large order). *When $n \in \mathbb{N} \to \infty$,*

$$J_n(x) = \frac{1}{n!}\left(\frac{x}{2}\right)^n\left(1 + \mathcal{O}\left(\frac{1}{n}\right)\right), \tag{C.6}$$

uniformly on compact subsets of $[0, +\infty)$,

$$H_n^{(1)}(x) = \frac{(n-1)!}{i\pi}\left(\frac{2}{x}\right)^n\left(1 + \mathcal{O}\left(\frac{1}{n}\right)\right), \tag{C.7}$$

uniformly on compact subsets of $(0, +\infty)$, and

$$J_n(x)H_n^{(1)}(x) = \frac{n}{i\pi}\left(1 + \mathcal{O}\left(\frac{1}{n}\right)\right), \tag{C.8}$$

uniformly on compact subsets of $[0, +\infty)$.

Proof. It can be obtained from the series representation of the functions J_n and $H_n^{(1)}$; see, e.g., [13, eqs. (3.97)–(3.98)]. ∎

We note that the estimates in Lemma C.4 are uniform on compact subsets of $[0, +\infty)$ for (C.6) and (C.8), and $(0, +\infty)$ for (C.7), i.e., the constants in the $\mathcal{O}$ are independent of both $n \to +\infty$ and x in that subset.

For the remaining lemmas, we will assume that all variables are defined as in sections 2 and 3. In particular,

$$\boldsymbol{y}_\epsilon = \lambda\epsilon^{-p}e^{i\theta_y}, \quad \boldsymbol{z}_\epsilon = \lambda\epsilon^{-q}e^{i\theta_z}, \quad 0 < p < q. \tag{C.9}$$

Lemma C.5. *When* $\epsilon \to 0^+$,

$$|\boldsymbol{y}_\epsilon - \boldsymbol{z}_\epsilon| = \lambda \epsilon^{-q} \left(1 - \epsilon^{q-p} \cos(\theta_y - \theta_z) + \mathcal{O}\left(\epsilon^{2(q-p)}\right)\right). \tag{C.10}$$

For any $\boldsymbol{x} = \lambda c_x e^{i\theta_x}$ *with* $c_x = \mathcal{O}(1)$, *when* $\epsilon \to 0^+$,

$$|\boldsymbol{x} - \boldsymbol{y}_\epsilon| = \lambda \epsilon^{-p} \left(1 - c_x \epsilon^p \cos(\theta_x - \theta_y) + \mathcal{O}\left(\epsilon^{2p}\right)\right). \tag{C.11}$$

Proof. We write

$$|\boldsymbol{y}_\epsilon - \boldsymbol{z}_\epsilon| = \lambda \epsilon^{-q} \left(1 - 2\epsilon^{q-p} \cos(\theta_y - \theta_z) + \epsilon^{2(q-p)}\right)^{1/2}. \tag{C.12}$$

Then, for small enough ϵ,

$$\left(1 - 2\epsilon^{q-p} \cos(\theta_y - \theta_z) + \epsilon^{2(q-p)}\right)^{1/2} = 1 - \epsilon^{q-p} \cos(\theta_y - \theta_z) + \mathcal{O}\left(\epsilon^{2(q-p)}\right). \tag{C.13}$$

We conclude by multiplying by $\lambda \epsilon^{-q}$. We obtain the result for $|\boldsymbol{x} - \boldsymbol{y}_\epsilon|$ by writing

$$|\boldsymbol{x}_\epsilon - \boldsymbol{y}_\epsilon| = \lambda \epsilon^{-p} \left(1 - 2c_x \epsilon^p \cos(\theta_x - \theta_y) + \epsilon^{2p}\right)^{1/2}. \tag{C.14}$$

∎

Lemma C.6. *When* $\epsilon \to 0^+$,

$$H_0^{(1)}(k|\boldsymbol{y}_\epsilon - \boldsymbol{z}_\epsilon|) = \frac{\epsilon^{q/2}}{\pi} e^{i\left(2\pi\epsilon^{-q}\left[1 - \epsilon^{q-p}\cos(\theta_y - \theta_z) + \mathcal{O}\left(\epsilon^{2(q-p)}\right)\right] - \pi/4\right)} \left(1 + \mathcal{O}\left(\epsilon^{q-p}\right)\right). \tag{C.15}$$

For any $\boldsymbol{x} = \lambda c_x e^{i\theta_x}$ *with* $c_x = \mathcal{O}(1)$, *when* $\epsilon \to 0^+$,

$$H_0^{(1)}(k|\boldsymbol{x} - \boldsymbol{y}_\epsilon|) = \frac{\epsilon^{p/2}}{\pi} e^{i(2\pi\epsilon^{-p}[1 - c_x\epsilon^p \cos(\theta_x - \theta_y)] - \pi/4)} \left(1 + \mathcal{O}\left(\epsilon^p\right)\right). \tag{C.16}$$

Proof. This is obtained by combining Lemma C.5 with Lemma C.3. ∎

Lemma C.7. *For any* $c_x = \mathcal{O}(1)$, *when* $\epsilon \to 0^+$,

$$\left\langle e^{-2i\pi(\epsilon^{-p}\cos(\theta_y - \theta_z) + c_x \cos(\theta_x - \theta_y))} \right\rangle = \frac{\epsilon^{p/2}}{\pi} \cos\left(2\pi\epsilon^{-p}\left[1 + c_x\epsilon^p \cos(\theta_x - \theta_z)\right] - \pi/4\right) \times \left(1 + \mathcal{O}\left(\epsilon^p\right)\right). \tag{C.17}$$

Proof. The integral on the left-hand side equals $J_0(2\pi h)$ with

$$h = \sqrt{(\epsilon^{-p}\cos\theta_z + c_x \cos\theta_x)^2 + (\epsilon^{-p}\sin\theta_z + c_x \sin\theta_x)^2}. \tag{C.18}$$

We then obtain an expansion for h and utilize Lemma C.3 for J_0. ∎

Lemma C.8. *For any* $\boldsymbol{x} = c_x \lambda e^{i\theta_x}$ *with* $c_x = \mathcal{O}(1)$, *when* $\epsilon \to 0^+$,

$$\tilde{v}_\epsilon^i(\boldsymbol{x}, \boldsymbol{y}_\epsilon, \boldsymbol{z}_\epsilon) = -\frac{\epsilon^{p/2}\epsilon^{q/2}}{4\pi^2 H_0^{(1)}(2\pi\epsilon)} e^{2i\pi(\epsilon^{-q} + \epsilon^{-p} - \epsilon^{-p}\cos(\theta_y - \theta_z) - c_x \cos(\theta_x - \theta_y) + \mathcal{O}(\epsilon^{q-2p}))} \times \left(1 + \mathcal{O}\left(\epsilon^{\min(p, q-p)}\right)\right) \tag{C.19}$$

and

$$\langle \tilde{v}_\epsilon^i \rangle(\boldsymbol{x}, \boldsymbol{z}_\epsilon) = -\frac{\epsilon^p \epsilon^{q/2}}{4\pi^3 H_0^{(1)}(2\pi\epsilon)} \cos\left(2\pi\epsilon^{-p}\left[1 + c_x\epsilon^p \cos(\theta_x - \theta_z)\right] - \pi/4\right) \times e^{2i\pi(\epsilon^{-q} + \epsilon^{-p} + \mathcal{O}(\epsilon^{q-2p}))} \left(1 + \mathcal{O}\left(\epsilon^{\min(p, q-p)}\right)\right). \tag{C.20}$$

Proof. We recall that

$$\tilde{v}_\epsilon^i(\boldsymbol{x},\boldsymbol{y}_\epsilon,\boldsymbol{z}_\epsilon) = -\frac{i}{4}\frac{H_0^{(1)}(k|\boldsymbol{y}_\epsilon-\boldsymbol{z}_\epsilon|)}{H_0^{(1)}(2\pi\epsilon)}H_0^{(1)}(k|\boldsymbol{x}-\boldsymbol{z}_\epsilon|). \tag{C.21}$$

The estimates are direct consequences of Lemmas C.6 and C.7. ∎

Lemma C.9. *When* $\epsilon \to 0^+$,

$$|\mu_\epsilon(\boldsymbol{y}_\epsilon,\boldsymbol{z}_\epsilon)^{-1}|^2 = \pi^2|H_0^{(1)}(2\pi\epsilon)|^2\epsilon^{-q}\left(1+\mathcal{O}\left(\epsilon^{q-p}\right)\right). \tag{C.22}$$

Proof. We recall that $\mu_\epsilon(\boldsymbol{y}_\epsilon,\boldsymbol{z}_\epsilon) = -H_0^{(1)}(k|\boldsymbol{y}_\epsilon-\boldsymbol{z}_\epsilon|)/H_0^{(1)}(2\pi\epsilon)$. Therefore,

$$|\mu_\epsilon(\boldsymbol{y}_\epsilon,\boldsymbol{z}_\epsilon)^{-1}|^2 = |H_0^{(1)}(2\pi\epsilon)|^2|H_0^{(1)}(k|\boldsymbol{y}_\epsilon-\boldsymbol{z}_\epsilon|)^{-1}|^2. \tag{C.23}$$

We use Lemma C.6 to get an expansion for $H_0^{(1)}(k|\boldsymbol{y}_\epsilon-\boldsymbol{z}_\epsilon|)^{-1}$ and its complex conjugate, and we utilize the fact that $|z|^2 = z\overline{z}$. ∎

Acknowledgments. We sincerely thank the members of the Inria Idefix and Makutu research teams, in particular Lorenzo Audibert, Hélène Barucq, and Florian Faucher, for fruitful discussions about inverse scattering problems and subsurface imaging. Florian also provided us with an earlier version of Figure 1. Finally, we extend our gratitude to Maxence Cassier and Christophe Hazard for their insights into the asymptotics for small scatterers.

REFERENCES

[1] M. Abramowitz and I. A. Stegun, *Handbook of Mathematical Functions with Formulas, Graphs, and Mathematical Tables*, Dover, New York, 1964.
[2] F. Alouges and M. Aussal, *FEM and BEM simulations with the Gypsilab framework*, SMAI J. Comput. Math., 4 (2018), pp. 297–318.
[3] L. Audibert and H. Haddar, *A generalized formulation of the linear sampling method with exact characterization of targets in terms of farfield measurements*, Inverse Problems, 30 (2014), 035011.
[4] L. Audibert and H. Haddar, *The generalized linear sampling method for limited aperture measurements*, SIAM J. Imaging Sci., 10 (2017), pp. 845–870.
[5] A. P. Austin and L. N. Trefethen, *Trigonometric interpolation and quadrature in perturbed points*, SIAM J. Numer. Anal., 55 (2017), pp. 2113–2122.
[6] G. Bao, S. Hou, and P. Li, *Inverse scattering by a continuation method with initial guesses from a direct imaging algorithm*, J. Comput. Phys., 227 (2007), pp. 755–762.
[7] F. Cakoni and D. Colton, *A Qualitative Approach to Inverse Scattering Theory*, Appl. Math. Sci., Springer, New York, 2014.
[8] F. Cakoni, D. Colton, and H. Haddar, *Inverse Scattering Theory and Transmission Eigenvalues*, CBMS-NSF Regional Conf. Ser. in Appl. Math. 88, SIAM, Philadelphia, 2016.
[9] M. Cassier and C. Hazard, *Multiple scattering of acoustic waves by small sound-soft obstacles in two dimensions: Mathematical justification of the Foldy–Lax model*, Wave Motion, 50 (2013), pp. 18–28.
[10] D. Colton, H. Haddar, and M. Piana, *The linear sampling method in inverse electromagnetic scattering theory*, Inverse Problems, 19 (2003), pp. S105–S137.
[11] D. Colton and A. Kirsch, *A simple method for solving inverse scattering problems in the resonance region*, Inverse Problems, 12 (1996), pp. 383–393.
[12] D. Colton and R. Kress, *Looking back on inverse scattering theory*, SIAM Rev., 60 (2018), pp. 779–807.
[13] D. Colton and R. Kress, *Inverse Acoustic and Electromagnetic Scattering Theory*, 4th ed., Springer, New York, 2019.

[14] D. Colton, M. Piana, and R. Potthast, *A simple method using Morozov's discrepancy principle for solving inverse scattering problems*, Inverse Problems, 13 (1997), pp. 1477–1493.
[15] A. Duroux, K. Sabra, J. Ayers, and M. Ruzzene, *Using cross-correlations of elastic diffuse fields for attenuation tomography of structural damage*, J. Acoust. Soc. Am., 127 (2010), pp. 3311–3314.
[16] L. C. Evans, *Partial Differential Equations*, 2nd ed., AMS, Providence, RI, 2010.
[17] T. Gallot, S. Catheline, P. Roux, J. Brum, N. Benech, and C. Negreira, *Passive elastography: Shear-wave tomography from physiological-noise correlation in soft tissues*, IEEE Trans. Ultrason. Ferroelectr. Freq. Control, 58 (2011), pp. 1122–1126.
[18] J. Garnier, H. Haddar, and H. Montanelli, *The linear sampling method for random sources*, SIAM J. Imaging Sci., 16 (2023), pp. 1572–1593.
[19] J. Garnier and G. Papanicolaou, *Passive Imaging with Ambient Noise*, Cambridge University Press, Cambridge, UK, 2016.
[20] O. A. Godin, N. A. Zabotin, and V. V. Goncharov, *Ocean tomography with acoustic daylight*, Geophys. Res. Lett., 37 (2010), L13605.
[21] P. Gouédard, L. Stehly, F. Brenguier, M. Campillo, Y. Colin de Verdière, E. Larose, L. Margerin, P. Roux, F. J. Sanchez-Sesma, N. M. Shapiro, and R. L. Weaver, *Cross-correlation of random fields: Mathematical approach and applications*, Geophys. Prospect., 56 (2008), pp. 375–393.
[22] I. Koulakov and N. Shapiro, *Seismic tomography of volcanoes*, in Encyclopedia of Earthquake Engineering, Springer, Berlin, 2014, pp. 1–18.
[23] N. Lebedev and R. Silverman, *Special Functions and Their Applications*, Dover, New York, 1972.
[24] H. Montanelli, *Numerical Algorithms for Differential Equations with Periodicity*, Ph.D. thesis, University of Oxford, 2017.
[25] H. Montanelli, M. Aussal, and H. Haddar, *Computing weakly singular and near-singular integrals over curved boundary elements*, SIAM J. Sci. Comput., 44 (2022), pp. A3728–A3753.
[26] H. Montanelli, F. Collino, and H. Haddar, *Computing singular and near-singular integrals over curved boundary elements: The strongly singular case*, SIAM J. Sci. Comput., to appear.
[27] K. G. Sabra and S. Huston, *Passive structural health monitoring of a high-speed naval ship from ambient vibrations*, J. Acoust. Soc. Am., 129 (2011), pp. 2991–2999.
[28] N. Shapiro, M. Campillo, L. Stehly, and M. H. Ritzwoller, *High-resolution surface-wave tomography from ambient seismic noise*, Science, 307 (2005), pp. 1615–1618.
[29] M. Siderius, H. Song, P. Gerstoft, W. S. Hodgkiss, P. Hursky, and C. H. Harrison, *Adaptive passive fathometer processing*, J. Acoust. Soc. Am., 127 (2010), pp. 2193–2200.
[30] E. A. Spence, I. V. Kamotski, and V. P. Smyshlyaev, *Coercivity of combined boundary integral equations in high-frequency scattering*, Comm. Pure Appl. Math., 68 (2015).
[31] L. N. Trefethen, *Approximation Theory and Approximation Practice*, extended ed., SIAM, Philadelphia, 2019.
[32] K. F. Woolfe, S. Lani, K. G. Sabra, and W. A. Kuperman, *Monitoring deep-ocean temperatures using acoustic ambient noise*, Geophys. Res. Lett., 42 (2015), pp. 2878–2884.
[33] G. B. Wright, M. Javed, H. Montanelli, and L. N. Trefethen, *Extension of Chebfun to periodic functions*, SIAM J. Sci. Comput., 37 (2015), pp. C554–C573.